Nanoscale

REVIEW

View Article Online
View Journal | View Issue

Cite this: *Nanoscale*, 2021, **13**, 9505

Graphene and water-based elastomer nanocomposites – a review

Christian N. Nwosu, [a] Maria Iliut [a] and Aravind Vijayaraghavan *[a,b]

Water-based elastomers (WBEs) are polymeric elastomers in aqueous systems. WBEs have recently continued to gain wide acceptability by both academia and industry due to their remarkable environmental and occupational safety friendly nature, as a non-toxic elastomeric dispersion with low-to-zero volatile organic compound (VOC) emission. However, their inherent poor mechanical and thermal properties remain a drawback to these sets of elastomers. Hence, nano-fillers such as graphene oxide (GO), reduced graphene oxide (rGO) and graphene nanoplatelets (GNPs) are being employed for the reinforcement and enhancement of this set of elastomers. This work is geared towards a critical review and summation of the state-of-the-art developments of graphene enhanced water-based elastomer composites (G–WBEC), including graphene and composite production processes, properties, characterisation techniques and potential commercial applications. The dominant production techniques, such as emulsion mixing and *in situ* polymerisation processes, which include Pickering emulsion, mini-emulsion and micro-emulsion, as well as ball-milling approach, are systematically evaluated. Details of the account of mechanical properties, electrical conductivity, thermal stability and thermal conductivity enhancements, as well as multifunctional properties of G–WBEC are discussed, with further elaboration on the structure–property relationship effects (such as dispersion and filler–matrix interface) through effective and non-destructive characterisation tools like Raman and XRD, among others. The paper also evaluates details of the current application attempts and potential commercial opportunities for G–WBEC utilisation in aerospace, automotive, oil and gas, biomedicals, textiles, sensors, electronics, solar energy, and thermal management.

Received 28th February 2021,
Accepted 10th May 2021

DOI: 10.1039/d1nr01324f

rsc.li/nanoscale

1. Introduction

Elastomers are a set of polymers that exhibit viscoelastic characteristics, with high elongation at break and low Young's modulus.[1,2] These distinctive properties coupled with their ease of processing and low-cost make them viable option for a wide range of applications.[3]

[a]*Department of Materials, The University of Manchester, Manchester M13 9PL, UK. E-mail: aravind@manchester.ac.uk*
[b]*National Graphene Institute, The University of Manchester, Manchester M13 9PL, UK*

Christian N. Nwosu

Christian Nlemchukwu Nwosu is a Ph.D. student in the Department of Materials at The University of Manchester. Previously, Christian was awarded his M.Sc. (2016) in Applied Nanotechnology from Cranfield University, UK, and a B. Sc. (2012) in Physics from Michael Okpara University of Agriculture, Umudike, Nigeria. His research is focused on the development of graphene-enhanced water-based elastomer nanocomposites and their applications.

Maria Iliut

Dr Maria Iliut is a post-doctoral research associate in the Department of Materials at The University of Manchester. She was awarded her Ph.D. (2013), M.Sc. (2010) and B.Sc. (2008) degrees from Babes-Bolyai University, Romania. Her research involves the development of graphene-enhanced elastomer nanocomposites. She is also the co-founder of Grafine, Ltd. She has published over 20 papers in international peer-reviewed journals.

WBEs are group of liquid-based elastomeric systems in aqueous (water) dispersions. This is in contrast to their conventional solvent-based elastomer (SBE) formulation counterparts. WBEs have been observed to possess outstanding characteristic properties in contrast to SBEs, such as (i) low to zero volatile organic compounds (VOCs) emission, (ii) low to zero toxicity and (iii) low flammability.[4,5]

Thus, WBEs are 'greener' (eco-friendly)[6] and advantageous towards occupational health and safety compared to SBE formulations, which are known for high VOCs emissions, flammability and toxicity. Hence, the use of SBE is currently limited due to several government regulations[7] in a bid to cut-down on its environmental pollution impacts, therefore creating the need for the formulation of WBEs. Thus far, natural rubber latex (NRL)[8–10] and its synthetic based form *cis*-1,4 polyisoprene (IPR)[11–14] remain the most widely studied WBEs, followed closely by formulations of water-based polyurethanes (wPU).[15] However, it is important to state that studies on water-based IPR (wIPR) are still not widely explored, compared to its solvent-based brands. Other forms of WBE, such as water-based silicone (wSi) and styrene–butadiene–rubber (wSBR), have also been reported,[16,17] but remain largely unexplored. Nevertheless, the vast majority of WBE are still at a developmental phase. These include the recently reported water-based ethylene–propylene–diene–monomer (wEPDM Trilene® T65) and similar latex formulations, such as polyacrylate rubber (ACM) and nitrile rubber (NBR) elastomeric systems by manufacturers.

On the contrary, the applicability of WBEs is presently constrained mostly due to their (i) poor mechanical properties, (ii) poor thermal properties and (iii) poor chemical (weatherability) properties[4,6] compared to their SBE counterparts.

This thus necessitates the need for the development of WBE composites in order to ensure proper utilisation of this set of elastomers in various (emerging) technological applications. To this effect, several filler materials have been employed for the improvement of WBE properties, such as cellulose nanocrystals[5,18] and silica.[6,19] Graphene is currently the strongest known material with superior mechanical properties (~1 TPa elastic modulus, ~130 GPa tensile strength and fatigue-life of $>10^9$ cycles at 71 GPa mean stress and stress range of 5.6 GPa),[20,21] outstanding thermal conductivity (~5300 W m^{-1} K^{-1}),[22] remarkable electronic properties (~200 000 cm^2 V^{-1} s^{-1} electron mobility)[23,24] and extraordinary electrical conductivity (~6000 S cm^{-1}).[25] Consequently, employing graphene nanofillers for the reinforcement of water-based elastomers will possibly improve their poor mechanical, thermal and chemical properties, as well as induce electrically conductive networks within the elastomeric chains. Thus, this leads to the development of a multifunctional high-performance WBE composite that meets several engineering applications.

Several reviews have documented the use of graphene nanofillers, such as graphene oxide (GO), reduced graphene oxide (rGO) and graphene nanoplatelets (GNPs), in conventional elastomer reinforcements,[26–28] as well as other carbon-based materials, such as carbon-nanotubes (CNTs), carbon black and graphite.[29] However, to date, there is no existing specific review on G–WBEC, possibly because this set of elastomers is still largely undergoing industrial development. Hence, the number of articles on this topic has seen an increase only in recent years, which is a strong indication that this is still an area of emerging research.

This review is focused on exploring specific developments on graphene enhanced WBE nanocomposites, with greater emphasis on their production techniques, properties, characterisation and potential applications.

Aravind Vijayaraghavan

Dr Aravind Vijayaraghavan is a Reader in Nanomaterials at The University of Manchester, where he leads the Nanofunctional Materials Group. He was an Alexander von Humboldt Fellow at Karlsruhe Institute of Technology and a Senior Postdoctoral Research Associate at Massachusetts Institute of Technology. He was awarded his Ph.D. (2006) and M.Eng. (2002) from Rensselaer Polytechnic Institute, USA and his B.Tech. from the Indian Institute of Technology, Madras, India in 2000. His research involves the science and technology of 2-dimensional materials for applications in sensors, composites and biotechnology. He has published over 100 papers in international peer-reviewed journals.

2. Graphene

Graphene, a monoatomic layer of graphite, is currently considered as the material for a wide range of robust disruptive technology. Hence, it has continued to attract wide attention from both academia and industry. Since its first isolation 17 years ago by Andre Geim and Konstantin Novoselov,[30] graphene (now widely referred as the building block of carbonaceous materials, such as CNT, fullerenes and graphite) has continued to provoke endless innovation in various areas of technology, such as composites,[31,32] quantum computation,[33] sensors, electronics, supercapacitors and medical applications.[33–35] However, it is worth noting that pristine graphene can not be stably dispersed in water[36] and is unfunctionalized as it lacks reactive groups, which should enhance its reactivity as pointed out by Liu *et al.*[37] In addition, its low-throughput and expensive nature[36] presents it as a complex material for integration into matrices, such as polymer composites. In lieu of these challenges, other derivatives of graphene, such as graphene oxide (GO), reduced graphene oxide (rGO), few-layer graphene (FLG) and graphene nanoplatelets (GNPs),

are currently being utilised for polymer composite reinforcement.

GO is graphene that has been chemically functionalised with oxygen-containing groups (possessing high oxygen content at ~2–3 carbon–oxygen ratio).[38] Hence, it is characterised by being reactive and hydrophilic, as such can easily be integrated into WBE matrices. Also, its reduced form (rGO) still has a higher degree of dispersibility and reactivity compared to pristine graphene. On the contrary, graphene-based materials (such as FLG and GNPs) comprise multiple graphitic sheets of 2–≥10, which are mostly non-oxygenated, unlike GO and rGO. However, FLG and GNPs can also be subjected to various sets of functionalisation depending on the required application. The bulk (multilayer) nature of this set of graphene derivatives, coupled with their possession of intrinsic properties of graphene, such as high electrical conductivity in contrast to GO, presents them as viable nanofillers for WBE nanocomposite production. On the other hand, FLG and GNPs are typically seen to possess poor dispersibility, which results in their agglomeration in the polymer matrix. As a result, they offer inhomogeneous reinforcement and require an additional dispersion medium for homogeneous integration into polymer matrices. The remarkable properties of graphene, as established by experimental investigations, are briefly summarised in Table 1, and fully discussed under section 2.1.

2.1. Intrinsic properties of graphene

An experimental investigation conducted by Lee *et al.* showed that monolayer graphene possesses ~1 TPa elastic modulus and ~130 GPa tensile strength.[20] This was found to be in agreement with the theoretical results later obtained by Liu *et al.* (~1 TPa elastic modulus and ~110 GPa tensile strength),[40] as well as mechanical characteristics (elastic modulus) previously reported for other carbonaceous materials, such as those for graphite[41] and single walled carbon nanotube (SWCNT).[42] Also, a recent report by Cui *et al.*[21] showed that graphene is capable of withstanding extreme fatigue conditions of $>10^9$ cycles at a mean stress of 71 GPa. Thus, graphene is currently viewed as the material for the revolution of the future composite industry *via* outstanding mechanical reinforcement, resulting in high-performance composites as initially investigated by Stankovich *et al.*,[31] among others.

Table 1 Some notable properties of graphene determined *via* experimental investigation

Properties		Experimental values	Ref.
Mechanical	Elastic modulus	~1 TPa	20
	Tensile strength	~130 GPa	
	Fatigue resistance	10^9 cycles at mean stress of 71 GPa	21
Thermal	Thermal conductivity	~5300 W m^{-1} K^{-1}	22
	Thermal stability	~2600 K	39
Electrical	Electrical conductivity	6000 S cm^{-1}	25

In addition, graphene remains the most thermally conductive material to date, capable of attaining ~5300 W m^{-1} K^{-1} conductivity value, as measured by Balandin *et al.*[22] *via* Raman optothermal probe for a monolayer graphene. However, this is in contrast to the low conductivity values reported for other carbonaceous materials.[43] Nevertheless, the attained experimental value of ~5300 W m^{-1} K^{-1} is still well below the theoretical predictions of ~8000 W m^{-1} K^{-1} and ~10 000 W m^{-1} K^{-1} reported by Nika *et al.*[44,45] and Evans *et al.*,[46] respectively. Also, a report by Kim *et al.*[39] indicates that monolayer graphene can withstand ≥2600 K temperature, thus demonstrating stronger thermal stability of graphene compared to those of metals. Furthermore, several experimental[47–50] and theoretical[45,51,52] studies have shown that factors, such as the grain-size, defect concentration, orientation, edge roughness, and impurities, tend to affect the graphene thermal conductivity. Hence, this remains an area of potential investigation towards harnessing the enormous thermal conductivity of graphene. Additional details on the graphene thermal conductivity can be accessed *via* previous reviews.[43,50,52,53]

To date, graphene remains the most conductive material ever measured with an electrical conductivity of about 6000 S cm^{-1}.[25] This is due to the relativistic behaviour of electrons found in graphene AB sub-lattices, which are capable of tunnelling through potential barriers. Several studies demonstrate that the electrical conductivity of graphene is directly proportional to temperature variations, but inversely proportional to its thickness (layers), implying that the electrical conductivity tends to increase with a rise in temperature, but drops with an increase in the number of layers.[54–56] Also, factors such as the orientation,[57] functionalisation[58,59] and lateral size[60] have been noted to offer a wide disruption to the electrical conductivity of graphene.

Some other properties of graphene include its outstanding barrier properties, being capable of stopping difficult-to-block gases, such as helium, especially when employed as a nanofiller in polymer composites. For instance, a recent study by Raine *et al.* noted a drastic reduction in the permeability of supercritical fluids, such as hydrogen sulphide (H_2S) and carbon dioxide (CO_2).[61] Also, studies by van Rooyen *et al.*[62] showed that graphene is capable of reducing the helium (He) permeability by 88%–96% when used as a nanofiller in a polymer matrix. Several other studies have also reported the remarkable barrier characteristics of graphene across various gaseous particulates, such as oxygen,[63,64] nitrogen, methane,[65] water vapour[66,67] and fuel-vapour transmission.[68] The available results thus demonstrate the great prospect of graphene as a barrier membrane in various industrial separation applications.

Additionally, several reports have shown that graphene possesses strong biomedical characteristics,[69–72] which are promising for the development of future medical therapeutics and drug delivery systems,[73–76] diagnostics,[77,78] tissue and organ engineering,[79] biosensing[80,81] and antimicrobial systems.[82–85] However, the graphene antimicrobial mechanism remains a contentious issue,[82,86] and is thus still subject to further inves-

tigation. Also, a majority of the current biomedical studies on graphene are based on the GO and rGO derivatives, possibly due to their oxidative stress features, which show strong relevance in biomedicine. Notwithstanding, a recent study by Lebre *et al.* shows that pristine graphene can trigger epigenetic changes in tissues *via* sustained induced innate immunity.[87] This report thus suggests the efficacy of graphene in biomedical systems.

Furthermore, studies on the chemical reactivity of graphene shows that monolayer graphene sheets are about 10 to 14 times more reactive compared to double or multilayer graphene.[88,89] Great changes in the chemical reactivity of graphene have been widely observed for its electron transfer (π–π) interactions with aryl diazonium salts,[88,90] and for radical addition reactions with compounds, such as benzoyl peroxide[89] and perfluorinated alkyl groups,[91] thus paving way for its facile tailored functionalisation. In addition, graphene edges are observed to be more reactive than its basal sheet.[92,93] Apart from the aforementioned reactions, which are majorly based on covalent chemistry,[37,94] graphene also undergoes non-covalent reaction with solvents, such as ionic liquids and polymers,[95–97] thus providing an opportunity for its wide range functionalisation and potential applications. Additionally, a theoretical study on graphene nanoribbons has shown that the reactivity of the armchair and zigzag oriented graphene is not directly proportional. Consequently, while the armchair increases in width, the zigzag structure decreases and *vice versa*.[98] However, the mechanism behind this claim remains largely unverified.

2.2. Properties of graphene-based materials

The GO graphene derivative is a functionalised form of graphene. Hence, it is reactive and can easily disperse in water and polymer matrices (being hydrophilic) due to its possession of most functional groups, such as hydroxyl (–OH) and epoxy groups on its "basal planes" and carboxyl (–COOH) or carbonyl functional groups on the film edges,[31] depending on the additives utilised in the functionalisation. The ease of dispersibility and exfoliation of GO into single sheets (monolayer GO) in various solvents makes it a viable nanofiller for polymer composites.[28] Furthermore, the presence of these oxidative functional groups renders GO as a poor electrical conductor with lower thermal stability,[28,99] as well as resulting in poor mechanical strength and inferior electrochemical electron transfer in GO-based graphene. Hence, to recover most properties of graphene, such as its conductivity, GO is mostly subjected to reduction process *via* either chemical,[100] thermal[101] or electrochemical[99] means, which yields the so-called rGO. The rGO exhibits moderate electrical conductivity with a reduction in solubility compared to GO.[34,102,103]

On the other hand, GNPs have been described by several authors as one with layers >10. However, there is still a lot of discrepancy on this subject matter, as several authors try to offer their own definition. For instance, Jang and Zhamu described GNPs as single-layer and multi-layer graphene derivatives.[104] This account was later modified by Bianco *et al.*, who referred to GNPs as graphite nanoplatelets, and multi-layer graphene (MLG) as those with 2–10 layers,[38] which Wick *et al.*[105] later referred to as FLG. This was further explained in the study conducted by Papageorgiou *et al.*, where the authors tried to provide some clarification on the subject, referring to FLG as those with the number of layers at between 2–5.[28] However, one remarkable fact to consider, based on previous reports in literature, is that GNPs are materials whose thicknesses lie below 100 nm. Thus, in this context, it might not be necessary to tie its nomenclature to the number of layers as it is clearly distinguishable from graphite, which is bulk 3D material. Also, based on the nomenclature released in 2017 by the International Organization for Standardisation (ISO), graphene and its derivatives were classified based on their constituent layers:[106] single layer graphene (SLG) referred to as graphene, 2 layers referred to as bilayer graphene (BLG), while 3–10 layers were referred to as FLG. Accordingly, Ye and Tour[106] suggested that GNPs are derivatives with layers beyond 10, which are usually obtained from the AB Bernal stacking of layers at room temperature. Nevertheless, this did not dispute the fact that graphene material nomenclature remains a task yet to be unravelled, especially in terms of the product characteristic uniformity; hence, the demands for a unique synergy amongst researchers and manufacturers in order to bridge the gap.

GNPs are usually produced *via* exfoliation techniques, achievable *via* thermal expansion or shear force applications, which weakens the van der Waals forces of attraction binding the graphene layers together,[106] similar to those employed for GO exfoliation. However, GO can best be classified as an oxidatively (chemically) functionalised graphene derivative[107,108] which are mostly assembled as monolayers,[108] unlike GNPs that comprise layers ≥10 (ref. 38) and are typically non-oxygenated. The exfoliation can be *via* application of heat, shear mixing, sonication, ball milling,[109] and by using carbondioxide, organic solvents and iron(II) acetate, which aids in the production of thick GNPs. Hence, it is being used for the wide-scale production of graphene,[106] especially for applications such as fillers in polymer composites.

2.3. Production of graphene

Graphene production for composites design and formulation is currently based on three broad routes, which are the wet-chemical route, liquid-phase route and gas-phase route. These routes can also be described as top-down approaches, and their graphene products are applicable for polymer composites development. Fig. 1 provides a general representation of graphene materials produced through these techniques.

2.3.1. Wet–chemical route

GO production. The GO route is a chemical process widely employed for the intercalation of bulk graphite, and its subsequent exfoliation into graphene sheets through chemical oxidation. This technique, which can also be referred to as wet-chemical synthesis,[120] is mostly based on procedures, such as Brodie's,[121] Staudenmaier's[122] and the widely acclaimed Hummers' method.[123] Hummers' approach is considered as less toxic and facile compared to the earlier methods. It can be utilised *via* various modifications, as demonstrated by

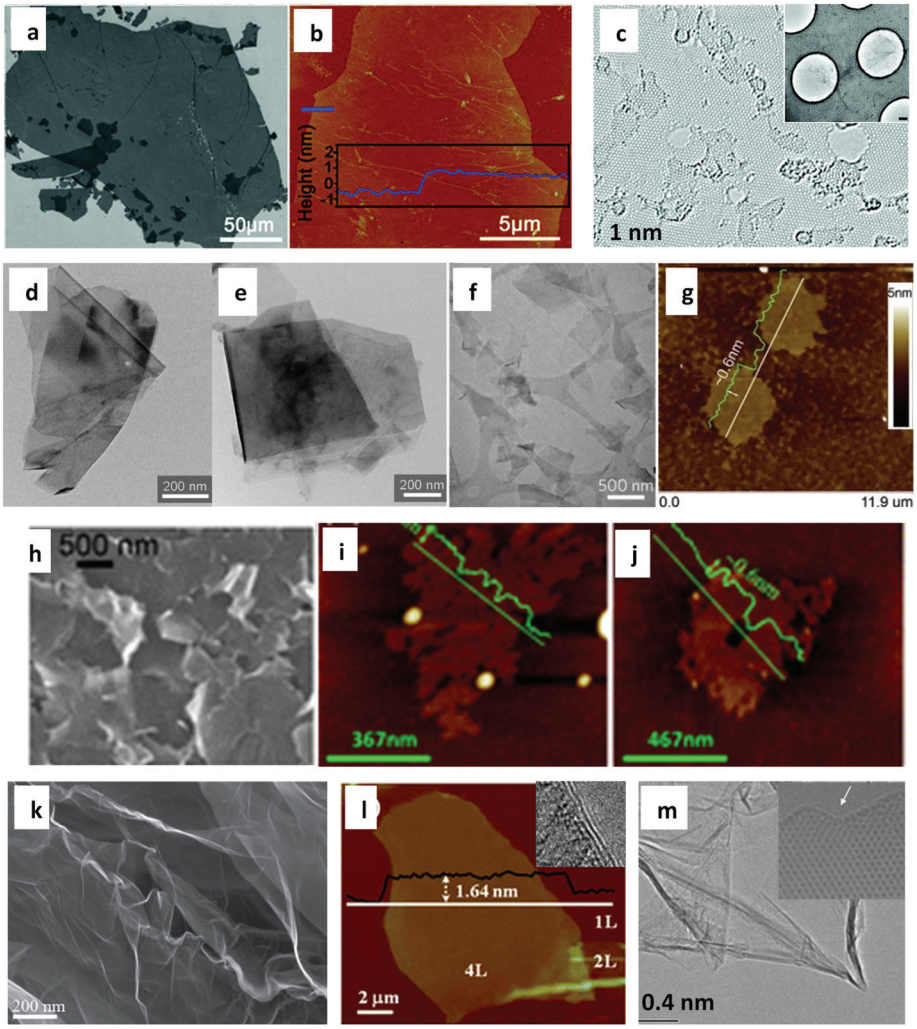

Fig. 1 Typical examples of graphene materials produced through different techniques: (a–e) graphene materials produced *via* wet-chemical route, (a) scanning electron microscopy (SEM) and (b) atomic force microscopy (AFM) micrographs of GO sheets (reprinted with permission from ref. 110. Copyright 2010 American Chemical Society), and (c) aberration-corrected transmission electron microscopy (TEM) micrograph of rGO (insert: TEM image of partly folded rGO sheets on a TEM grid) prepared through GO route (reprinted with permission from ref. 111. Copyright 2010 American Chemical Society), (d and e) graphene materials produced *via* electrochemical exfoliation, TEM micrographs of (d) anodic exfoliates and (e) cathodic exfoliates (reprinted with permission from ref. 112. Copyright 2015 Elsevier); (f–l) graphene produced *via* liquid-phase route, (f) TEM micrograph of graphene nanosheets prepared using a high-shear mixer (reprinted with permission from ref. 113. Copyright 2014 Nature Publishing Group), (g) AFM micrograph of FLG sheets prepared using a kitchen blender (reprinted with permission from ref. 114. Copyright 2014 Elsevier), (h) SEM micrograph of graphene flakes prepared *via* sonication exfoliation in NMP (reprinted with permission from ref. 115. Copyright 2014 American Chemical Society), (i and j) AFM micrographs of liquid-exfoliated graphene dispersed in water *via* sonication (reprinted with permission from ref. 116. Copyright 2013 Royal Society of Chemistry), (k) SEM micrograph of graphene flakes produced *via* jet cavitation (reprinted with permission from ref. 117. Copyright 2017 Taylor & Francis), (l) AFM micrograph of graphene prepared *via* ball-milling (insert: high resolution TEM (HRTEM) image highlighting folded edge) (reprinted with permission from ref. 118. Copyright 2013 Royal Society of Chemistry); and (m) TEM micrograph of graphene flakes produced using the gas-phase technique (insert: HRTEM highlighting flake edge) (reprinted with permission from ref. 119. Copyright 2009 Royal Society of Chemistry).

different research groups.[102,124,125] The approach also leads to the production of oxygenated graphene with dominant hydroxyl, carboxyl and epoxide groups (Fig. 2). Current efforts are geared towards achieving the large-scale commercial production of GO by exploring various processes, such as microbial oxidation,[126,127] electrochemical oxidation,[128,129] thermal oxidation[130] and hydrothermal oxidation.[131] A recent review by Brisebois and Siaj[132] provided a clear state-of-the-art account on GO production processes.

GO reduction. Due to the need to harness the remarkable electrical properties inherent in graphene for specific applications, most of the oxygenised functional groups in GO (such as the –OH, –C–O–C and –COOH groups) are partly sacrificed *via* various processes, such as chemical[100] or thermal[133] reduction routes (Fig. 3), thus giving rise to the reduced form of graphene oxide (rGO).[34,100,134–136]

Electrochemical exfoliation. Electrochemical synthesis is currently being explored as one of the easy routes to scale up gra-

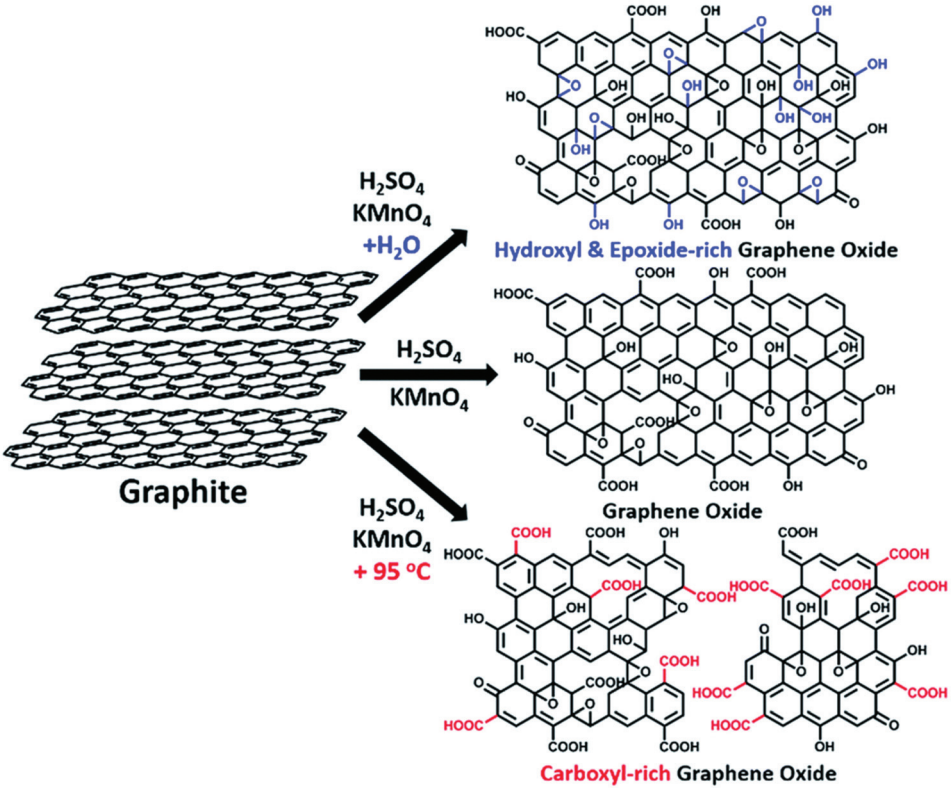

Fig. 2 GO synthesis *via* modified Hummers' method, highlighting the controlled species of functional groups that can be achieved by employing this wet-chemical process.[124]

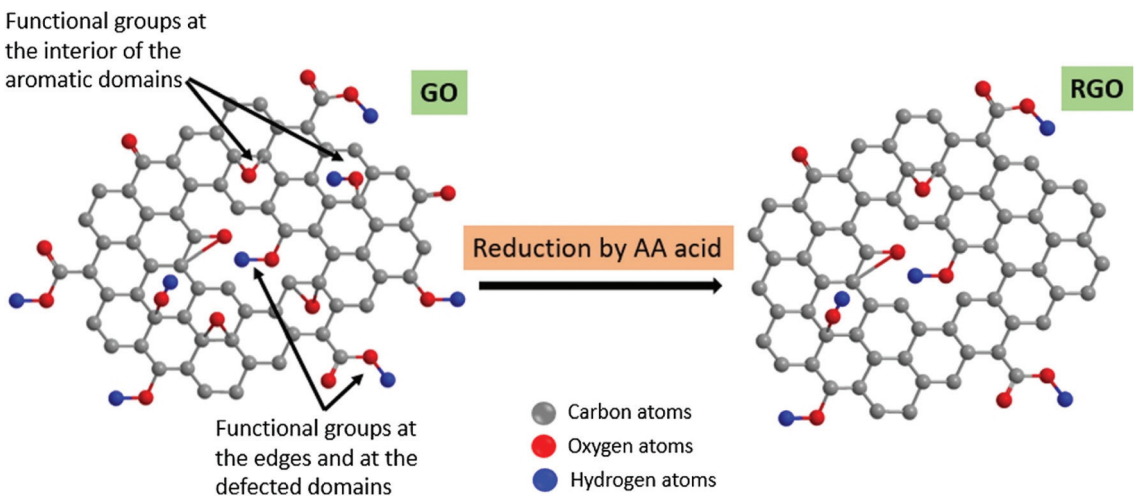

Fig. 3 Schematic description of rGO production from GO using ascorbic acid (vitamin C), showing the removal of the functionalised oxygen species originally dominant in GO. Reprinted with permission from ref. 103. Copyright 2018 Elsevier.

phene production due to its ease of processing, good-scalability, fast-delivery, safe and eco-friendly nature based on the available literature reports.[112,128,137–142] This method is similar to the GO route (earlier discussed), as it also employs aqueous acidic solutions (Fig. 4a), such as H_2SO_4 and H_3PO_4. However, it is worth noting that ionic liquids, such as inorganic salts,[138] aqueous and non-aqueous liquids,[143] are widely employed here as electrolytes.[138,140,142,143] Hence, this technique is not heavily reliant on strong chemicals, as obtainable in the GO wet-chemical process. Electrochemical synthesis is usually conducted *via* two different ways, cathodic-reduction and anodic-oxidation,[143] which respectively leads to the production of

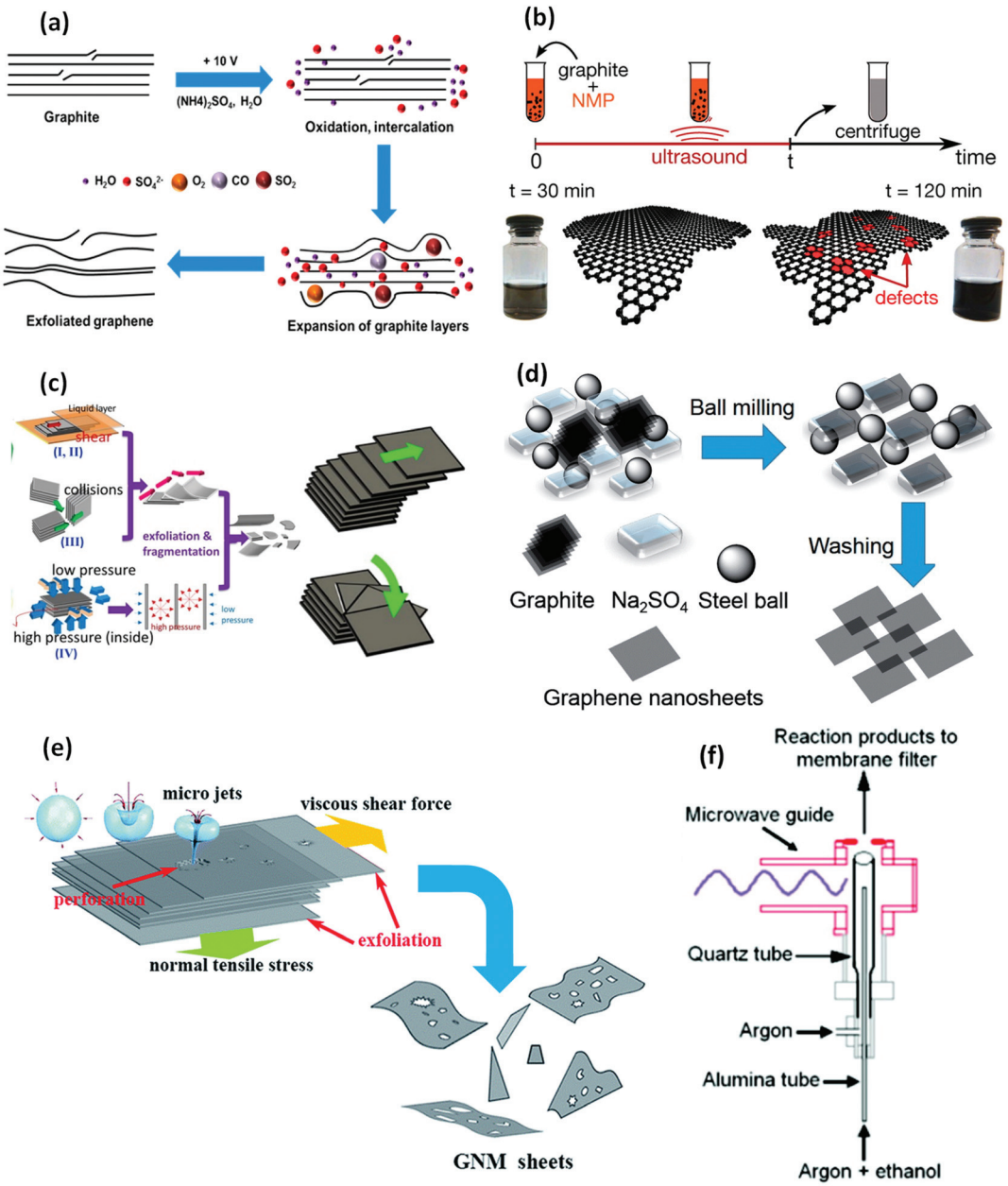

Fig. 4 Illustration of graphene production *via* different exfoliation techniques: (a) schematic description of the electrochemical exfoliation mechanism of graphene using an inorganic salt-based aqueous electrolyte solution, such as $(NH_4)_2SO_4$. Reprinted with permission from ref. 138. Copyright 2014 American Chemical Society. (b) Description of the graphene production process *via* sonication exfoliation (highlighting the effects of sonication time on the graphene sheets). Reprinted with permission from ref. 115. Copyright 2014 American Chemical Society. (c) Highlighting the shear exfoliation mechanism of graphene production (graphene sheets being dispersed *via* translational and rotational lateral exfoliation). Reprinted with permission from ref. 114. Copyright 2014 Elsevier. (d) Schematic of graphene production using ball–mill (highlighting ball-milling of graphite powder using $NaSO_4$ as a dispersant). Reprinted with permission from ref. 144. Copyright 2014 Royal Society of Chemistry. (e) Jet cavitation mechanism of graphene sheet exfoliation *via* micro-jets induced shear force. Reprinted with permission from ref. 145. Copyright 2014 Royal Society of Chemistry. (f) Representation of the atmospheric pressure MPR gas phase system utilised for graphene production. Reprinted with permission from ref. 146. Copyright 2008 American Chemical Society.

unfunctionalized graphene sheet and functionalised electrochemical graphene oxide (EGO).[137] A drawback to this technology includes the expensive nature of ionic liquids and use of strong electrolytes.[143] A review by Low *et al.*[143] provides a more succinct account of this technique.

2.3.2. Liquid–phase route. Liquid-phase exfoliation (LPE) employs mainly organic, ionic and non-ionic solvents for the exfoliation of graphene *via* sonication,[115,147–158] high-shear,[113] and ball-milling exfoliation,[159–161] as well as microfluidisation (jet-cavitation)[117,162,163] technique, which is closely associated

with high-shear exfoliation. These approaches involve the combination of both mechanical and chemical or electrical energy. LPE techniques are generally viewed as the most facile and eco-friendly routes towards the large-scale and low-cost production of graphene-based materials.

As a non wet-chemical route, LPE leads to the production of mostly monolayer and multilayer graphene sheets,[164] which are highly conductive with inherent properties of pristine graphene.[20,22,30,165,166] In this technique, graphite precursors undergo intercalation within the dispersed liquid medium, which results in the breakdown of the van der Waals forces binding the graphitic layers together, exfoliating into graphene sheets.

Sonication exfoliation. Sonication exfoliation utilises ultrasound to break down the weak van der Waals bonds tying the Bernal-stacked graphitic layers, and thus the exfoliation of the layers in a solvent. Subjecting these weakly exfoliated layers through centrifugation completely separates the graphitic layers into distinct graphene sheet dispersions. However, care must be taken in order to avoid inducing so much stress on the π–π covalently bonded graphene structure, which might result in induced defects.[115,154] Also, sonication has been observed to encourage the generation of graphene rich in carboxyl and ether/epoxide functional-groups.[154] Ultrasonication is usually conducted *via* two major routes: bath-sonication[153] and horn (tip/probe) sonication[152] (Fig. 4b). A horn sonicator generates ~10-fold of the power compared to a bath sonicator. Hence, the horn sonicator has been noted to be more efficient and less time-consuming. However, bath sonication is favoured for exfoliation of mild homogenous systems, while horn sonication is mostly utilised for multi-layered systems, such as pristine graphite.[167]

High-shear exfoliation. Exfoliation by high-shear mixing utilises mechanical shear to break down bulk graphite into graphene sheets within a suitable dispersing medium (such as organic or inorganic solvenst and ionic liquids) (Fig. 4c). Here, the rate of exfoliation largely depends on several factors, such as the dispersing liquids surface–energy, viscosity, and density, as well as the shear processing conditions like shear-speed, time, mixer head and rate of centrifugation employed. This technique is considered as largely facile and scalable. Hence, it is being vigorously explored for large-scale graphene production. On the contrary, despite the remarkable merits of this technique, graphene produced *via* this method can suffer induced stresses because of the shear localisation within the rotor–stator or rotating blade cavity. Fabrication of a special shear–mixer for graphene exfoliation, capable of achieving full scale turbulence within the entire high-shear regions by overcoming high-shear localization, will possibly help to ameliorate this challenge.[168]

Ball–mill exfoliation. Ball–mill exfoliation (BME) is currently gaining wide attention due to its possibility of generating a shear-force dominated mill for the facile breakdown of the π–π stacked graphitic sheets van der Waals forces.[169] BME provides an easy route towards the rapid exfoliation of graphite, and hence, the high graphene production scalability compared to other LPE techniques. BME works in principle through the generation of shear and collision forces, which leads to ball-milling (grinding) of the graphite powder, by overcoming the van der Waals forces binding the graphitic layers together through edge-opening,[118] resulting in its intercalation and exfoliation (Fig. 4d). Subjecting the resultant exfoliated graphitic-sheets to centrifugation leads to their full exfoliation and separation into graphene sheets/nanoplatelets (GNPs).[170] BME is generally carried out through two different paths: wet ball-milling[159,160] (employing liquid solvents) and dry ball-milling,[118,171] utilising either planetary or stirred-media ball–mill technology. The impacts of collision force remain a source of concern for this technology due to the possibility of fragmentation and basal-defects inducement at high-energy milling since the prevention of grinding media collision is inevitable.[168,172]

Jet-cavitation. In view of the aforementioned challenges, several studies are currently exploring other LPE techniques, such as jet-cavitation or micro-fluidisation, which involves the use of high-pressurised fluids[173] to break down graphite flakes and exfoliate the graphitic layers into graphene sheets dispersion (Fig. 4e). This is basically conducted through electro-hydraulic pump suction and compression motions. Fluids, such as water[174] and surfactants, as well as supercritical fluids like CO_2,[175] are mostly employed in jet cavitation. Although this technique achieves high shear-rate without shear localisation, its limitation includes the possibility of microfluidic channel blockage, especially for graphite flake sizes exceeding 100 μm.[173]

2.3.3. Gas-phase route. Presently, the gas-phase route is also widely explored for the production of high-quality graphene sheets,[176,177] having been first introduced in 2008 by Dato *et al.*[146] Some studies indicate that this approach reportedly leads to the production of high-quality, ordered and stable graphene sheets.[119,176]

Gas-phase graphene (GPG) production is largely achieved using microwave plasma reactors (MPR) (under atmospheric pressure) (Fig. 4f). Here, the carbon-precursor is first introduced into the MPR chamber, followed by precursor decomposition by MPR generated Argon plasma, even without the need for substrates,[146] solvents or catalysts. Hence, the gas-phase route can be considered as facile and more eco-friendly since it generates only gases (such as H_2 and CO) as by-products.[176] It is worth noting that the deployment of gas-phase graphene for various applications, such as composites reinforcement, is still largely underexplored. However, the continual growth in lab-scale production of GPG will perhaps pave the way to its wide range applications in the future.[176] In addition, unlike other graphene production routes (such as LPE and wet-chemical routes that results into high-throughput production), GPG currently achieves low production yield, which remains an unresolved obstacle to the growth of this technology. A simplified comparison of the various graphene processing routes and their achievable graphene characteristics are provided in Table 2.

Table 2 Comparison of wet-chemical, LPE and gas-phase graphene production routes and their associated graphene properties

Technique		Graphene property	Merits	Demerits
Wet-chemical route	GO route	a. Oxygen-functionalised hydroxyl, carboxyl, carbonyl and epoxide groups	a. High-throughput graphene production	a. Employs mainly strong chemicals
		b. Highly insulating	b. Facile synthesis of oxygenised graphene	b. High-volume of toxic chemical wastes
		c. Disordered structure	c. Possibility of achieving covalently functionalised graphene	c. Involves multiple processing steps
		d. Can easily be functionalised or reduced	d. Scalable	
	Electrochemical exfoliation	a. Electrochemical functionalised GO (EGO) *via* anodic oxidation; with sp^3 defect		
		b. Monolayer graphene *via* cathodic reduction; wrinkled		
Liquid-phase route	Sonication exfoliation	a. Monolayer, few-layer and multilayer graphene	a. High-throughput graphene production	a. Employs mainly ionic and organic solvents
		b. Conductive	b. Possibility of achieving various forms of non-covalent graphene functionalisation	b. High-cost of ionic liquids
		c. Functionalised or non-functionalised graphene	c. Facile and scalable	c. Possibility of liquid waste generation
		d. Possibility of disordered graphene		
	High-shear exfoliation; ball–mill exfoliation	a. Monolayer, few-layer and multilayer graphene		
		b. Conductive		
		c. Functionalised or non-functionalised graphene		
		d. Possibility of fractured graphene		
	Jet-cavitation	a. Monolayer, few-layer and multilayer graphene		
		b. Conductive		
Gas-phase route	Microwave plasma exfoliation	a. Monolayer, few-layer and multilayer graphene	a. Facile and scalable	a. Low-throughput production
		b. Conductive	b. Possibility of large-scale production of pure and highly ordered graphene sheets	b. Generation of carbon monoxide gas
			c. No chemical or liquid solvent required; hence, it is eco-friendly as there is no liquid waste to the environment	

2.4. Global graphene production and supply

A recent report indicates that the global production capacity of graphene is most likely up to 2.5 kilotonnes per annum since 2018, with demand currently accumulated to ~400 tonnes per annum (well above the previous estimate of ~50 tonnes per annum) (Fig. 5).[178] Thus, this is a clear indication that the graphene production supply currently outstrips its demand; hence, a great advantage for its application for industrial product development, such as G–WBEC formulations.

A study by Döscher *et al.* also pointed out that the existing global supply of graphene majorly hinges on factors, such as stable demand growth (expected to be stronger as its industrial application increases), possibility of global production capacity stagnation (need for improved and low-cost production methods), gradual fall in the cost of production (mainly dependent on the production volume), pricing strategy (dependent on economic pressure or conscious efforts towards market shares capitalisation), grade improvement (consistency in the quality of produce), as well as market consolidation. In addition, it is worth noting that the supply inconsistency and lack of standards in graphene manufacturing remain a critical factor restricting its industrial advancement.[178] This can be enhanced possibly *via* the development of a graphene innovation ecosystem and the provision of an adequate innovation support.[179]

Also, graphene materials (such as GNPs), which are typically employed for large-scale applications, are presently priced at a cost of 100–700 € per kg, while GO-based graphenes (GO and rGO) are currently sold at higher costs of ~2500 € per kg. However, experts estimate that the cost of GNPs will fall to ~20 € per kg by 2022 (about 60% reduction in cost against the earlier estimate of ~50 € per kg predicted to be achieved by 2025). This is a clear indication of the rapid progress in the graphene production capacity, being far below the earlier estimate of ~50 € per kg, initially projected as the most sustainable price for the large-scale utilisation of graphene. In addition, more progress is expected down the line as the price of high-quality GNPs are expected to drop further by 2030 to ~25 € per kg, while lower-grade flakes are expected to drop below 8 € per kg for massive industrial uptakes.[178]

2.5. Toxicity and environmental impact of graphene materials

The utilisation of strong chemicals in most graphene material production methods remains a demanding challenge to the environment. For instance, the use of H_2SO_4 and hydrazine in

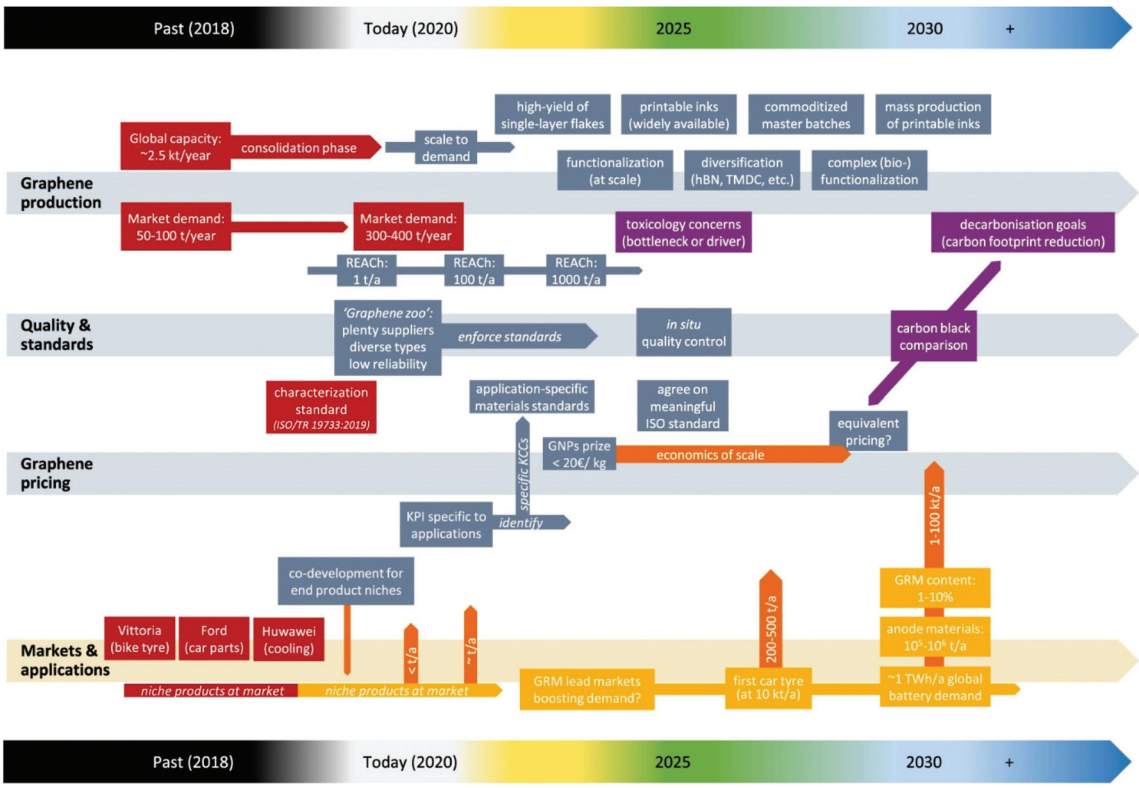

Fig. 5 2020 graphene materials industrialisation roadmap (experts estimate between 2018 and beyond). The specific progress analysis is highlighted in red colour, purple colour indicates the critical challenges, other colours indicates future actions and estimations.[178]

GO and rGO synthesis have been widely criticised, as these reagents pose a serious ecological threat to humans, terrestrial and aquatic environments. Thus, they could trigger freshwater eco-toxicity, cancer effect on humans, as well as NO_x emissions.[180] In addition, the utilisation of organic solvents, such as sodium dodecylsulphate (SDS) and sodium dodecylbenzenesulphonate (SDBS) in FLG/GNPs production,[151,156,160] remains a possible cause for human[181] and environmental concern. Hence, there is urgent need to harness more eco-friendly solvents and techniques in graphene materials production. This have been demonstrated in few reports using safe and eco-friendly routes like thermal reduction process and non-hazardous substances, such as ascorbic acid (vitamin C)[103] and glucose[182] for rGO synthesis, and thus eradicating the harmful environmental impact of toxic reagents like hydrazine.

On the other hand, the available studies on the dermal toxicity of graphene-based composites demonstrate that graphene does not induce toxic effects to the human skin. For example, a study on polypropylene–fumarate/polyethylene glycol–GO (PPF/PEG–GO) nanocomposites showed no induced toxicity on exposure to human dermal fibroblast.[183] Also, a study on GO-coated cotton fabric exhibited no irritation to skin tissues (demonstrated on rabbit skin), even though it was able to inactivate 98% of bacteria within <4 hours exposure.[184] Similarly, another report employing polyvinylpyrrolidone-coated GO (PVP–GO) on human immune cells (*in vitro*), such as macrophages, T lymphocytes and dendritic cells, showed that the PVP–GO composite exhibits good immunological biocompatibility effects.[185] This is in agreement with a recent *in vitro* study on skin irritation, where Fusco *et al.*[181] demonstrated that graphene materials (GO, rGO and FLG) do not induce skin irritation upon exposure to reconstructed human epidermis based on the SkinEthic™ test. However, skin irritation was observed for FLG processed with organic solvents, such as sodium dodecyl sulphate (SDS).[181] On the contrary, a similar *in vitro* study on the toxicity of graphene materials on HaCaTs human skin keratinocytes indicates that GO and FLG were able to induce slight differential effects on the HaCaTs cells.[186] Thus, this demonstrates a direct correlation with recent results obtained by Pulingam *et al.*, where a similar study on HaCaT cells showed that the GO toxicity effects on skin cells are majorly dose-dependent and appears to be negligible at <100 μg ml^{-1} concentration.[187]

In addition, a recent cytotoxicity study (conducted *via* both *in vitro* and *in vivo*) on G–WBEC utilising the FLG/natural rubber (FLG–C–NR) nanocomposite revealed that graphene incorporation within the NR matrix does not compromise its biocompatibility, as no sign of toxicity, nor skin irritation was observed for up to 48 hours exposure.[188] However, the majority of the available literature results suggests that graphene toxicity (as well as its susceptible environmental effects) is largely attributable to the overall nature of the surface chemistry (functionalised sites, especially the reactive oxygen species dominant in the derivatives, such as GO), particle size,

number of layers, concentration of the graphene material,[189,190] and the processing techniques employed in the graphene production.[180]

Notwithstanding, the available experimental data is still a subject of debate and divergence of opinion, as there appears to be significant gaps in the literature yet to be filled.[191] Also, there seems to be limited studies on the toxicity of pristine graphene, as well as GNPs, since most of the available investigations are generally focused on GO-based graphene. However, the issue of graphene toxicity as it is today can better be described as a "double-edged sword of risks and exploitable opportunities", as graphene materials (such as GO) have been found to exhibit antimicrobial and anti-cancer properties.[192] Thus, graphene materials could find a wide range of applications in biomedical engineering.

Furthermore, the end-of-life cycle (carbon footprint) of graphene-based composites, such as G–WBEC, is envisaged to occur through either particle emission, or leaching *via* landfills.[191,193] However, experts suggest that the mass transport of graphene flakes through the rubber matrix is unlikely, considering the large size nature of graphene flakes and their non-volatility.[191] In addition, there are concerns around organic pollutant emission through the weathering of rubber composites being ascribed to graphene. Nevertheless, this remains yet to be investigated.[191] However, a preliminary study on the enzymatic biodegradation of GO and rGO-based graphene (in the presence of veratryl alcohol) using *lignin peroxidase* (LiP) (an enzymatic discharge of white rot fungus) showed that LiP is capable of degrading these graphene materials efficiently. Hence, the abundance of white rot fungus in nature means that there is high potential for the efficient degradation of graphene[194] at end-of-life without posing a significant environmental risk. In addition, there appears to be no available study on the environmental risk associated with G–WBEC, possibly because of their widely acclaimed eco-friendly nature. Yet, there is need for multi-scale investigation for a better understanding of graphene materials, as well as the G–WBEC end-of-life cycle mechanism.

Finally, the concern about toxicity and the end-of-life cycle impact of graphene materials remains a puzzle yet to be fully resolved. A recent expert analysis anticipates the issue of graphene material toxicity to be fully resolved by 2025, while its end-of-life cycle impact in terms of the carbon footprint on the environment is expected to be addressed in the years ahead from mid-2030 and beyond (Fig. 5).[178] Although these concerns are presently seen as both justified and perceived issues, they remain one of the major obstacles limiting the massive deployment of graphene materials in various products. Hence, resolving this challenge would possibly trigger a tsunami in the demand for graphene materials for large-scale industrial applications, being that graphene-based systems appear promising for the replacement of more toxic products that are presently widely available in the market.[178] Because this challenge of graphene toxicity and its end-of-life environmental concern scenarios to humans, terrestrial and aquatic habitats remains yet to be unravelled, this topic would continue to be an issue of controversy. Hence, there is a need for a coordinated, multi-centred and collaborative investigation towards unravelling this challenge facing graphene industrialisation.

3. Graphene enhanced water-based elastomer composites (G–WBEC)

The performance of WBE is still riddled with inefficient engineering properties, as they have been found to possess poor mechanical and thermal properties, as well as high susceptibility to water and chemical attacks.[6] Thus, WBE performs poorly compared to traditional SBE. Therefore, there is a need to improve the properties of WBE in order to ensure their applicability as high-performance engineering elastomers.

Several filler materials have been employed for the reinforcement of WBE. For instance, Lin *et al.*[195] used cellulose-nanofibers for the reinforcement of wPU. They found an improvement in both Young's modulus and tensile strength, while the elongation at break was found to decrease with a rise in the cellulose nano-fibre content. Also, Lei *et al.*[5] recently employed office-waste processed cellulose nanocrystals for wPU reinforcement, and achieved better thermal stability with ~2–20 °C delay in the degradation temperature. Similarly, Zhang *et al.*[196] achieved better hardness, thermal stability and improved water-resistance for silica-reinforced wPU. Likewise, a significant increase in both soft-segment and hard-segment glass-transition temperatures (T_{gs}) were observed in the zinc–oxide reinforced wPU nanocomposite, as the ZnO content increased from 0–5%,[197] while a ~14.9 MPa rise in the tensile strength was observed for 1 wt% clay reinforced wPU.[198] A similar improvement in the mechanical properties and thermal stability has also been widely reported for NRL and IPR through reinforcement with fillers, such as silica,[199–202] starch,[203] calcium carbonate,[204] clay,[205] and cellulose nanofiber.[206]

Nevertheless, carbonaceous materials (such as carbon black and CNTs) are largely being employed for WBE reinforcement with greater improvement in both mechanical and thermal properties, such as those reported for NRL and IPR-based elastomeric composites.[207–212] Apart from improving on the mechanical and thermal properties of the WBE, CNTs also aid in transforming the originally insulating elastomers into electrically conductive films,[213–215] unlike other organic nanofillers discussed earlier. For instance, Kuan *et al.*[214] reported a ~26 °C difference in the thermal stability improvement and 370% tensile strength enhancement for the multiwalled CNTs/wPU composite.

However, with the discovery of graphene, more studies are now focusing on its application for the engineering of high-performance and multifunctional elastomer composites. This is largely due to its unrivalled mechanical, thermal, and electrical properties, coupled with its high surface-to-volume ratio and low cost of the parent material (graphite)[216] compared to CNTs[217] and other known materials. Hence, recent studies have shown the possibility of graphene utilisation as a nanofiller for WBE reinforcement. Although *pristine* graphene is not being employed due to its inertness and high hydrophobicity to water, graphene derivatives (such as GO and rGO[218–220]) are

mostly utilised for WBE composites design due to their easy interaction with polymeric molecules. On the contrary, the use of a GNP derivative for WBE composites formulation remains virtually non-existent at present. The reason for this poor use of GNPs in WBE is not yet properly understood, although it might be due to its hydrophobic nature, unlike GO and rGO graphene-based materials.

In addition, apart from graphene/NRL composite formulations that have been widely investigated, a study on graphene-based wIPR composite formulations appears to be virtually unavailable. A recent patent by Leng *et al.*[221] on graphene/polyisoprene latex composites remains the only visible work highlighting the use of graphene in wIPR reinforcement. In fact, work on synthetic polyisoprene graphene composites is majorly concentrated on the *trans*-1,4 polyisoprene isomer, which is not relevant for elastomeric applications. The cause of this under-utilisation of graphene in wIPR reinforcement remains a question yet to be unravelled, and hence presents an opportunity for more research in this area of study.

3.1. G–WBEC production techniques

The preparation of graphene–elastomer composites takes into consideration certain processing factors, such as the time duration and cost of the production technique. However, each technique employed infers special dispersion characteristics and thus, a distinct form of resultant nanocomposite.[28] Hence, achieving a homogenous dispersion of the filler–matrix blends will ensure a proper load transfer within the WBE matrix.[99] Two major routes are currently being explored for the preparation of G–WBEC: emulsion mixing (solution blending) and *in situ* emulsion polymerisation.[216,217] In addition, ball-milling is currently being investigated for G–WBEC processing. Fig. 6 gives a brief description of these techniques being exploited for G–WBEC production.

3.1.1. Emulsion mixing (blending). This technique involves the integration of an aqueous polymer (such as WBE) and graphene dispersion. Subsequently, the elastomer and graphene–dispersion mixture is thereafter blended together *via* stirring, ultrasonication or shear mixing using either high-shear or low-shear. The resultant hybrid-system is possibly degassed (in order to remove the available bubbles usually trapped within the mixture) and cast into films or mould. Thereafter, it is subjected to drying for water evaporation, leaving behind the graphene–elastomer nanocomposite film.[216,219,222]

Depending on the graphene derivative employed in the process, surfactants or surface modifications are mostly employed in preparing GNPs dispersions prior to blending (emulsion mixing), while aqueous GO dispersions are normally reduced to rGO after the blending process.[216] Post-blending reduction of the GO will no doubt ensure a properly dispersed filler–matrix system due to the predominant GO hydrophilic functional groups. On the contrary, pre-functionalisation of GNPs prior to emulsion-mixing will also aid in its dispersion within the elastomeric matrix since GNPs are not mostly hydro-

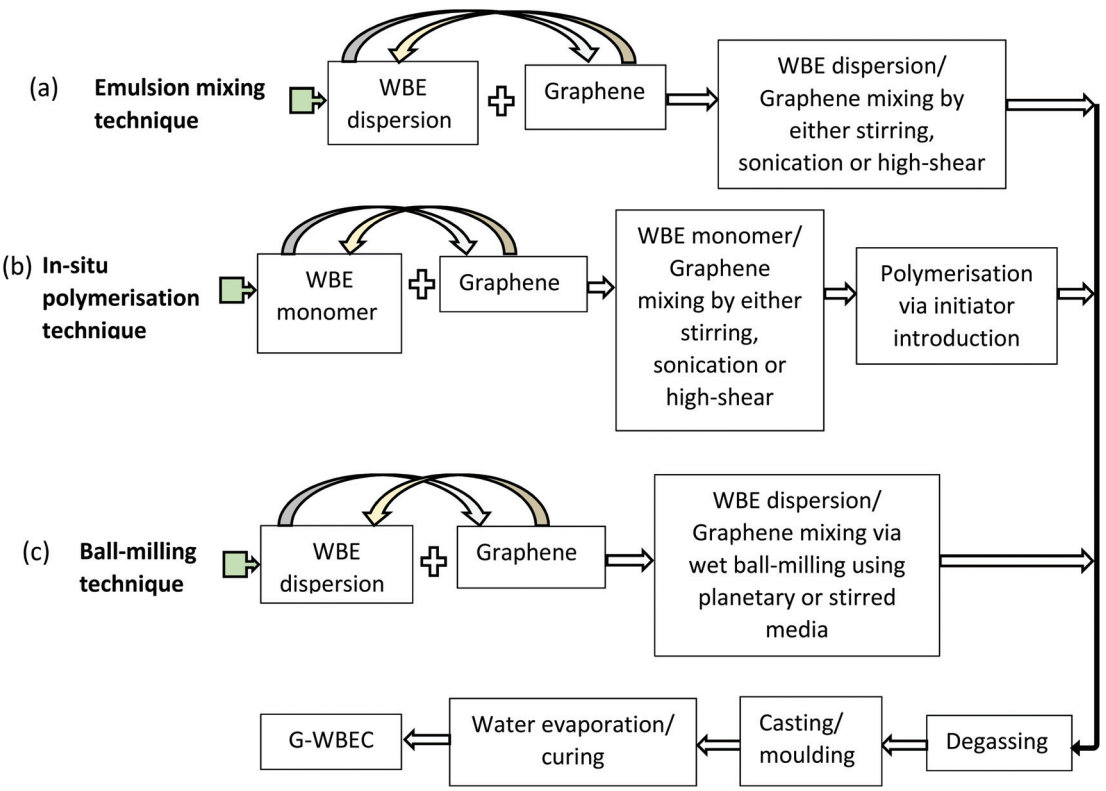

Fig. 6 Schematic representation of the steps involved in G–WBEC production techniques: (a) emulsion mixing technique, (b) *In situ* polymerisation technique, and (c) ball-milling technique.

philic in aqueous systems. Though the reduction of GO to rGO can also be realised prior to blending with WBE, contrary to post-blending reduction process. However, this mostly leads to certain degree of rGO gel-like agglomerates formation in contact with WBE dispersion, majorly due to rGO hydrophobic nature. Hence, the choice of GO reduction strategy largely depends on the research question and applicability. As presented above, Fig. 7a shows the process of GO integration with wPU and its subsequent reduction to rGO; Fig. 7b highlights the rGO/wPU nanocomposite molecules interfacial interaction, while Fig. 7c illustrates the aqueous GNP/polymer dispersion interactions. The evaporation of water can be conducted under atmospheric conditions or under high temperature using a vacuum oven. After evaporation, cured composite films can be utilised for extrusion (melt moulding), compression moulding, blow-moulding, or injection-moulding.[216,218] This technique can also be referred to as solution or latex mixing process. However, WBEs are devoid of solvents, unlike most solution/latex-based elastomer formulations.

Emulsion mixing is widely explored for graphene–elastomer nanocomposites processing. This is possibly due to it being facile and requiring less processing time. It also provides the opportunity to tailor the polymer properties prior to mixing.[223] On the other hand, a major limitation of this technique is the

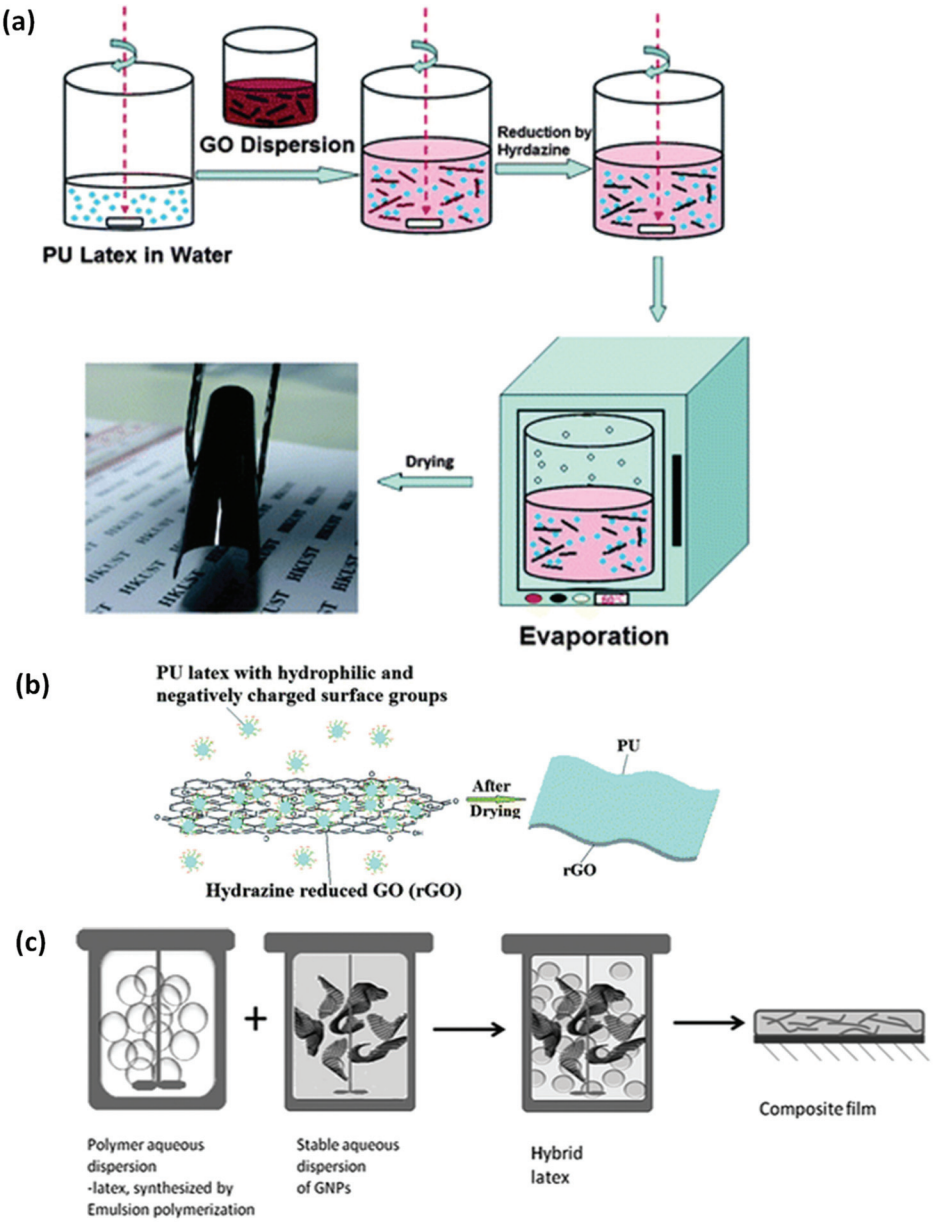

Fig. 7 Schematic description of emulsion mixing: (a) highlights emulsion mixing process of rGO with the wPU latex, (b) describes the mechanism of rGO interaction with wPU molecules. Reprinted with permission from ref. 219. Copyright 2012 Royal Society of Chemistry. (c) Illustration of the emulsion mixing of GNPs with aqueous polymer dispersions. Reprinted with permission from ref. 216. Copyright 2016 Wiley-VCH Verlag GmbH & Co.

possibility of graphene flake re-agglomeration upon water removal (evaporation).[99] To solve this problem, several studies have suggested blending by hetero-coagulation or self-assembly *via* electrostatic impulse through which the hybrid dispersion can be separated into aqueous and composite phases.[17,224] However, the coagulation process, which is mostly used for latex elastomers (such as NRL), requires the use of flocculants, such as HCl,[225] which might introduce some chemical residues within the fabricated G–WBEC. Spasevska *et al.* employed emulsion mixing for graphene/polymer composite processing with the aid of an aqueous polyurethane cross-linker, and achieved a 14-fold increase in the elastic modulus with significant electrical conductivity characteristics.[223] A similar study utilised this technique and achieved significant improvement in the gas barrier permeability of the rGO/NRL composite.[226] Also, Iliut *et al.* employed this technique in developing rGO/wPU and rGO/NRL composites, and achieved a >50% rise in the elastic modulus with some increase in the elongation to break at 0.1 wt% graphene loading of wPU and NRL elastomers.[218] In addition, recent report by Bernard *et al.* achieved an increase of about 200% and 300% in the elastic modulus and tensile strength, respectively, with a rise of 38% in the thermal conductivity and 43% reduction in flammability[222] for the GO/wPU composite prepared *via* emulsion mixing. Therefore, this technique, which can also be described as latex technology process,[221,227] remains the most viable, scalable and environmentally friendly option for G–WBEC production.

3.1.2. *In situ* polymerisation. The quest to overcome agglomeration challenges in emulsion mixing and ensure stronger covalent bonding of the graphene/polymer interface might have perhaps led to the exploration of *in situ* polymerisation.[228] This technique involves the synthesis of graphene and WBE *via in situ* polymerisation. Conventionally, emulsion polymerisation starts with the surfactant emulsification of the hydrophobic monomer, and thus the introduction of a water-soluble phase. Initiator thermolysis and the addition of the first monomer units in the aqueous phase lead to the generation of free radicals, which triggers polymerisation.[217] However, this is not the case for WBEs since they are already hydrophilic, so it does not necessarily require surfactant emulsification. Therefore, WBE reinforcement with graphene nanofillers for composite formulation is a more facile and direct approach, as graphene derivatives (such as GO) are already hydrophilic, except for rGO and GNPs, which might require the use of surfactant stabilisers.

The *in situ* polymerisation synthesis is mostly supported by sonication, which assists in breaking the monomers into small-droplets. This technique offers an opportunity for the proper dispersal of graphene flakes within the polymer matrix prior to polymerisation, and thus better dispersion.[216,228] Hence, this majorly results in an improved mechanical property of the composite. In addition, this method creates the space for the development of more homogeneous graphene/elastomer composites with unique morphologies,[216] unlike the emulsion mixing technique. Several numbers of studies have demonstrated the use of an *in situ* polymerisation technique for G–WBEC production. Hu *et al.* employed this technique for the processing of the rGO/wPU nanocomposite, and noted good dispersibility and stability of rGO with a consistent increase in the mechanical property for 2 mass% rGO loading, as well as improvement on the flame retardancy and smoke suppression.[220] Also, the study by Lee *et al.*[229] on GNSs/wPU *via in situ* emulsion polymerisation produced well-dispersed graphene flakes within the wPU matrix with an observed improvement on the mechanical and electrical properties of the wPU. It is interesting to note that the graphene nanosheets (GNSs) reported in these studies are no other derivative, but rGO. However, this shows that GO and rGO are the most widely studied graphene derivatives with this technique.

The *in situ* polymerisation technique can also be modified into other forms of formulation processes, such as mini-emulsion polymerisation (which employs high-shear to breakdown monomers into very small droplets),[230] microemulsion polymerisation (involves the addition of >10 wt% surfactant and co-surfactants into aqueous monomer dispersions, and thus reduces their interfacial surface energy)[232] and Pickering polymerisation (which involves the use of oil-phase systems, such as *para*-xylene).[233] Fig. 8 provides a brief description of the *in situ* polymerisation process. Details about these procedures have been documented in the study by Arzac *et al.*[216] and Bourgeat-Lami *et al.*[217]

However, it is worth noting that a series of drawbacks exist while employing this technology. For instance, the technique is not viable for the production of NRL/graphene nanocomposites since NRL exists mainly as a one-part elastomeric dispersion, and hence requires no initiator to blend with graphene fillers with the exception of its synthetic IPR.[234] Also, this method tends to encourage the sticking of graphene flakes within the polymer macromolecular-chains, resulting in a restricted interconnecting network formation, and thus leading to poor electrical conductivity.[228] On the contrary, it offers a great mechanical property advantage. A comparative study between emulsion mixing and *in situ* polymerisation techniques has been investigated by Arzac *et al.*, where the authors concluded that emulsion mixing favours electrical conductivity, but is poor in the mechanical property reinforcement (mostly due to weakly bonded graphene flakes). In contrast, *in situ* polymerisation was reported to yield a strong covalent bond between the graphene fillers and polymer molecules, thus resulting in a decrease in the electrical conductivity.[228]

3.1.3. Ball-milling. The available reports show that remarkable results can also be achieved by employing the ball-milling technique in processing graphene/elastomer composites.[235,236] However, it is worth noting that the utilisation of this technique for the production of G–WBEC remains heavily underutilised. Nevertheless, this technique is quite promising for G–WBEC production since it can be employed *via* either wet or dry mode. The wet-mode can easily be adapted for graphene incorporation into WBE with efficient milling control; hence, the possibility of obtaining improved exfoliation and dispersion of graphene flakes within the elastomeric matrix.

This technique has been employed specially for the processing of GNP-based polymer composites, as demonstrated for

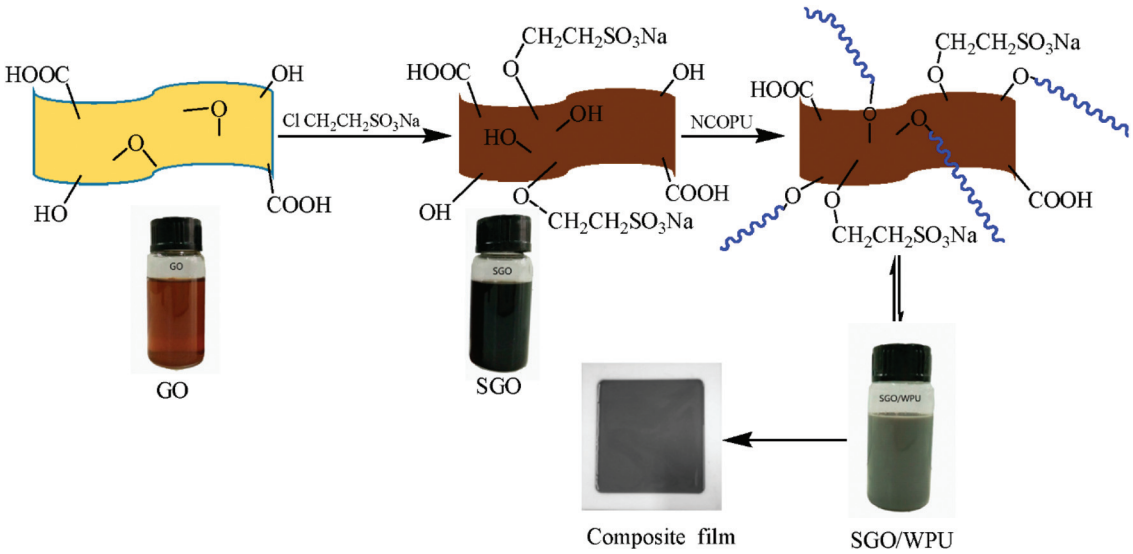

Fig. 8 Schematic description of *in situ* polymerisation of the sulfonated graphene oxide (SGO)/wPU nanocomposite.[231]

the GNP/TPU[236] and GNP/V-PDMS composite formulations.[235] Thus, the results obtained by Xu *et al.*[235] and those by Chen and Chen[236] indicate that this technique offers a great mechanical property advantage in elastomeric composites compared to other known techniques, such as the emulsion mixing (high-shear and sonication) method. Therefore, it infers that ball-milling is worth employing for G–WBEC processing, especially where good mechanical property enhancement is desired.

Nevertheless, the challenge of high compression forces (impact or contact forces) remains one of the major drawbacks to this technology, as these forces easily result in the crumpling of graphene flakes, thus affecting their efficient dispersion within the elastomeric matrix. Therefore, there is a need to fine-tune the processing parameters by ensuring efficient shear-force dominance over compressive forces during milling,[235] which will possibly lead to further improvement in the general property of the composite, particularly its electrical property.

Finally, in addition to the merits and demerits of any specific technique, as summarised in Table 3, it is also necessary to consider the application or research interest, while choosing a technique to employ in the G–WBEC formulation.

3.2. Properties and characterisation of G–WBEC

Studies conducted so far show that graphene is capable of improving the properties of elastomers of water-based origin. This improvement is majorly observed in the areas of mechanical and thermal properties, as well as the induction of electrical conducting channels within the elastomeric matrix. Furthermore, the properties of G–WBEC are observed to be highly dependent on:

- Processing technique
- % graphene loading
- Graphene derivative
- Functionalisation
- Nature of the elastomeric material
- Processing conditions employed
- Rate of graphene dispersion within the elastomeric matrix

For instance, Kinloch *et al.*[237] recently noted that nanomaterial dispersion within a composite matrix is highly reliant on the desired property in terms of application. Thus, high-filler loading in the direction of the load is mostly desired in mechanical property enhancement, which is contrary to the

Table 3 Brief summary of the effects of emulsion mixing, *in situ* polymerisation and ball-milling techniques in G–WBEC production

Processing technique	Merits	Demerits
Emulsion mixing	• Good filler/matrix interface • Unrestricted network interconnection • Excellent electrical property • Low-cost and facile process	• Lack of excellent dispersion • Moderate mechanical property
In situ polymerisation	• Excellent filler/matrix interface • High mechanical properties • Moderately cost-effective	• Restricted interconnected network formation • Moderate electrical conductivity • Multi-step process
Ball-milling	• Good mechanical property • Facile processing • Higher-scalability	• Possibility of graphene flake crumpling • Possibility of poor filler dispersion • Moderate electrical property • Moderately expensive nature of ball–mill machine

electrical property improvement, where the low-filler loading concentration is mostly desired in order to achieve a random percolated network. However, the microstructures required for achieving multifunctional properties remain rather complicated.[237] Consequently, the combination of these aforementioned factors determines to a great extent the graphene/WBE matrix interface reinforcement, which in effect, regulates the behaviour of the formulated composite material as highlighted in Tables 4–6. Again, it is important to note that apart from relatively few works focusing majorly on the mechanical, thermal, and electrical properties of G–WBEC, there tends to be no significant study yet on the barrier and weatherability properties of this set of composites.

Additionally, to date, wPU and NRL dominate this area of research, followed slightly by wSi. This is possibly because NRL remain the major non-synthetic source of WBE, while wPU and wSi currently remain the most widely developed synthetic WBEs compared to other groups of WBEs, which are largely still at the formulation and developmental stage. Hence, there exists a huge vacuum in this area of study. Another hurdle yet to be addressed in this area of research is the issue of poor industrial scalability of this set of composites, mainly due to the low industrial throughput of graphene-based materials production and their associated cost as required for WBE reinforcements.

3.2.1. Mechanical properties. The impact of graphene nanofillers on WBE has been shown to improve their elastic modulus, tensile strength and elongation to break. For instance, Kim and Kim achieved about a 623% increase in the wPU modulus at 1 wt% GO reinforcement, with ~105.4% and ~43.16% reduction in elongation to break and tensile strength, respectively (Fig. 9a).[238] Similarly, Zhou *et al.* reported a ~1245.36% increase in the modulus of poly(3,4-ethylenedioxythiohene):poly(styrene sulfonic acid)-modified wPU with a ~330% reduction in the elongation to break at a rGO loading of 1 wt% (Fig. 9b).[239] Furthermore, up to a 706% rise in the wPU tensile strength was reportedly obtained in a previous study by Hu and Zhang at a 2% mass loading of rGO.[220] In addition, a recent study by La *et al.* noted about a 10-fold increase in the abrasion resistance, as well as a ~400%, 200% and 30% increase, respectively, for the elongation to failure, tear strength and tensile strength of the GNP/NRL composite.[240] However, it is worth noting that a majority of the results obtained so far (using GO and rGO) were largely achieved through emulsion mixing or *in situ* polymerisation. Notwithstanding, similar studies have shown that the ball-milling technique is also a promising approach towards realising the good mechanical property reinforcement in G–WBEC, especially where GNPs are being employed.[235,236]

However, achieving these improvements is not a straightforward approach. The final product depends largely on the formulation processes as outlined earlier, which largely determines the rate of graphene dispersion and consequent load transfer within the elastomeric matrix. Hence, obtaining a simultaneous improvement in the elastic modulus, tensile strength and elongation to break remains a herculean task because an increase in the modulus (as the % graphene loading increases) possibly leads to a reduction in the tensile strength and elongation to break, and *vice versa*, as highlighted in Table 4. Thus, more effort should be concentrated towards developing a complementarity of properties, which is largely application-dependent.

Nevertheless, apart from the tensile-test analysis, some other tests have also shown the reliability of graphene in the mechanical property improvement of WBE. For instance, a recent study by Kale *et al.* achieved a ~0.22% improvement in the abrasion resistance of wPU through the 0.2 wt% loading of silica-functionalised GO.[241] Some other tests that have proven the mechanical property enhancement of elastomeric systems with graphene include: (i) a fatigue study of graphene/NRL,[242] (ii) puncture investigation of graphene/NRL,[243] and (iii) dynamic mechanical analysis of graphene/wPU composites.[244]

The above mechanical test investigations are clear indications that graphene nanofillers can serve not only for the improvement of the elastic modulus and tensile strength, but can also boost the abrasion resistance of WBE. Also, graphene-based materials offer a greater possibility for the enhancement of the tear strength, fatigue life, puncture, creep, flexure and impact resistance of WBE. However, it is worth noting that the mechanical tests conducted on WBE so far remain limited, with a majority of the tests focusing mainly on tensile tests. Hence, to ensure the reliability of G–WBEC, there is a need to explore various sets of mechanical tests in future studies.

3.2.2. Thermal properties. The introduction of graphene nanofillers into WBE has been demonstrated to significantly boost their thermal stability, as well as thermal conductivity. However, the studies so far (as summarised in Table 5) show that no significant work has been conducted on the thermal conductivity of G–WBEC formulations, with the exception of graphene/NRL based composites. The reason for this vacuum is yet unknown, although the performance of graphene materials in the thermal stability enhancement of WBE has been quite remarkable. For instance, the integration of 2 phr value of few-layer graphene-sheets (FGS) into the wPU emulsion resulted in a ~24.7 °C rise in the decomposition temperature at 50% weight loss,[245] while a study by Kale *et al.*[241] showed a ~44.48% rise in the decomposition temperature of wPU at 0.2% GO–silica reinforcement (Fig. 10).

Also, studies by Lim *et al.*[246] and Potts *et al.*[224] showed that an increase of up to 36.42% and 39.49% in the thermal conductivity of NRL is realisable through 0.1 phr and 5 wt% rGO reinforcement, respectively. In addition, a similar investigation by George *et al.*[247] demonstrated the possibility of achieving a ~483% rise in the thermal conductivity of NRL at 1.5 phr loading of FLG. Some other results obtained through similar studies are highlighted in Table 5.

3.2.3. Electrical conductivity. Employing graphene in WBE generates electrically conductive channels within the elastomeric network. Thus, this demonstrates the possibility of developing the smart electronic materials of the future. Available studies have shown that it is possible to achieve significant electrical conductivity in WBE using graphene, as highlighted in Table 6. Equally, investigation by Yousefi

Table 4 Mechanical properties of G–WBEC prepared using different graphene-based materials and their associated production routes

Elastomer	Graphene derivative	% Graphene loading	Processing Technique	Elastic modulus (increase/decrease) (MPa)	% Modulus (increase/ decrease)	Tensile strength (increase/decrease) (MPa)	% Tensile strength (increase/decrease)	% Elongation at break (increase/ decrease)	Ref.
wPU	FGS (rGO nanosheets)	2 phr	*In situ* polymerisation	~20.3	~25.5	~−14.1	~−65.28	−138	229
wPU	FGS	2 phr	Emulsion mixing (sonication)	~2 (at 10% strain)	~10	−2.2	~−11.96	−95	245
wPU	GO	4 wt%	Emulsion mixing (sonication)	NA	NA	8.7	47.28	~−575	248
wPU	GO	2% mass	Emulsion mixing (high-shear)	400	200	13	100	~250	222
wPU	GO	1 wt%	Emulsion (stirring)	137.7	~623	−16.1	~−43.16	−105.4	238
wPU	GNSs (rGO nanosheets)	2 phr	Emulsion mixing (sonication)	~−10.3	~−15.56	~6.6	~22.3	~−21	249
wPU	rGO	2% mass	Emulsion mixing (*in situ*)	NA	NA	~19.6	706	NA	220
wPU–acrylate	PDMS-modified GO	0.1 wt%	*In situ* polymerisation	NA	NA	−0.379	−68.91	~482.92	250
wPU	Functionalised GO	2 wt%	*In situ* polymerisation	NA	NA	5.22	~138.83	~−15.8	251
wPU	Silica modified GO	0.2%	Emulsion mixing	NA	NA	20	~100	−36.59	241
wPU/ PEDOT:PSS[a]	rGO	1 wt%	Emulsion mixing	~227.9	~1245.36	NA	NA	−330	239
wPU	rGO	0.1 wt%	Emulsion mixing (high-shear)	NA	NA	4.31	~33.65	~3.69	218
NRL	rGO	2 wt%	Emulsion mixing	NA	NA	8.1	47.37	−15	252
NRL	FLG	1.5 phr	Emulsion mixing	~0.4	~25	~9.9	~39.6	−49	247
NRL	rGO	0.9 phr	Emulsion mixing	1.75	~154.9 (at 300% modulus)	8.11	~50.2	NA	253
NRL	GO	0.08 wt%	Emulsion mixing (high-shear)	NA	NA	3.33	~35.61	80.45	218
NRL	TRGO dispersed in SDS	3 phr	Emulsion mixing	~1.35	~168.75 (at 100% modulus)	~4.56	~23.38	−152	254
NRL	GO	0.1 phr	Emulsion mixing	NA	NA	~7	~40	NA	255
NRL	GO	5 wt%	Emulsion mixing	NA	NA	5.65	~369.28	−137	256
NRL	rGO	0.1 phr	Emulsion mixing	NA	NA	2.23	~7	−15	246
NRL	rGO	5 wt%	Emulsion mixing	NA	NA	NA	NA	−90	224

[a] PEDOT:PSS = poly(3,4-ethylenedioxythiohene):poly(styrene sulfonate); NA: not available.

Table 5 Thermal properties of G–WBEC prepared using different graphene-based materials and their associated production routes

Elastomer	Graphene derivative	% Graphene loading	Processing technique	Thermal stability	Thermal conductivity	Ref.
wPU	FGS	2 phr	Emulsion mixing (sonication)	~24.7 °C increase in the decomposition temperature (at 50% weight loss)	NA	245
wPU	GO	2 wt%	Emulsion mixing (sonication)	~18.6 °C increase in the decomposition temperature	NA	248
wPU	GO	1.2–2 wt%	Emulsion mixing (high-shear)	21 °C increase in the decomposition temperature	0.1 W m^{-1} K^{-1}; 38% increase	222
wPU	Allyl isocyanate modified GO (iGO)	1 wt%	Emulsion mixing	~23.8 °C increase in the decomposition temperature (at 30% weight loss)	NA	244
wPU–acrylate	PDMS-modified GO	0.1%	*In situ* polymerisation	25 °C increase in the decomposition temperature (at 5% weight loss)	NA	250
wPU	OH-functionalised GO (fGO)	2 wt%	*In situ* polymerisation	~1200% improvement in the flame retardancy	NA	251
wPU	Silica modified GO (GOSI)	0.2 wt%	Emulsion mixing	~44.48 °C increase in the decomposition temperature (at 10% weight loss)	NA	241
NRL	FLG	1.5 phr	Emulsion mixing	NA	0.379 W m^{-1} K^{-1} (483% increase at 23 °C)	247
NRL	GO	5 wt%	Emulsion mixing	9.1 °C increase in the decomposition temperature	NA	256
NRL	rGO	0.1 phr	Emulsion mixing	NA	0.236 W m^{-1} K^{-1} (36.42% increase at 40 °C)	246
NRL	rGO	5 wt%	Emulsion mixing	NA	0.219 W m^{-1} K^{-1} (39.49% increase)	224

NA: not available.

Table 6 Electrical properties of G–WBEC prepared using different graphene-based materials and their associated production routes

Elastomer	Graphene derivative	Graphene loading	Processing technique	Percolation threshold	Electrical conductivity increase (S cm^{-1})	Ref.
wPU	GNSs (rGO nanosheets)	2 wt%	*In situ* polymerisation	~2 wt%	6.146×10^{-10}	229
wPU	FGS	2 phr	Emulsion mixing (sonication)	2 phr	$\sim 1.039 \times 10^{-7}$	245
wPU	rGO	2 wt%	Emulsion mixing (magnetic stirrer)	0.078 vol%	$\sim 4 \times 10^{-4}$	219
wPU	GNSs (rGO nanosheets)	2 phr	Emulsion mixing (sonication)	NA	$\sim 1.31 \times 10^{-5}$	249
wPU/PEDOT:PSS	rGO	1 wt%	Emulsion mixing	NA	~5.7	239
NRL	GNP	NA	Emulsion mixing	NA	$\sim 3.54 \times 10^{-12}$	257
NRL	FLG	1.5 phr	Emulsion mixing	NA	2.75×10^{-6}	247
NRL	TRGO-B (prepared by Brodie's method)	4 wt%	Emulsion mixing	NA	10^{-4}	258
NRL	TRGO dispersed in SDS	3 phr	Emulsion mixing	NA	$\sim 10^{-6}$	254
NRL	rGO (GO *in situ* reduction with hydroiodic acid)	5%	Emulsion mixing	NA	$\sim 1 \times 10^{-2}$	256
NRL	rGO (GO *in situ* reduction with hydroiodic acid)	5 vol%	Emulsion mixing	0.31 vol%	4.93×10^{-1}	259

PEDOT:PSS = poly(3,4-ethylenedioxythiohene):poly(styrene sulfonate); TRGO-B = thermally reduced graphite oxide produced by Brodie method; NA: not available.

et al.[219] showed that an increase of $\sim 4 \times 10^{-4}$ S cm^{-1} in the conductivity of wPU is realisable using 2 wt% rGO (Fig. 11). Also, Zhou *et al.*[239] reported an increase of ~5.7 S cm^{-1} in the wPU/poly(3,4-ethylenedioxythiohene):poly(styrene sulfonic acid) conductivity, achieved at 1 wt% rGO loading.

Remarkably, a majority of the available studies so far tend to focus more on rGO-based graphene materials in contrast to GO and GNPs. The reason for this might be because of the poor conductivity nature of GO and the dispersion challenges associated with GNPs within polar-based systems, such as

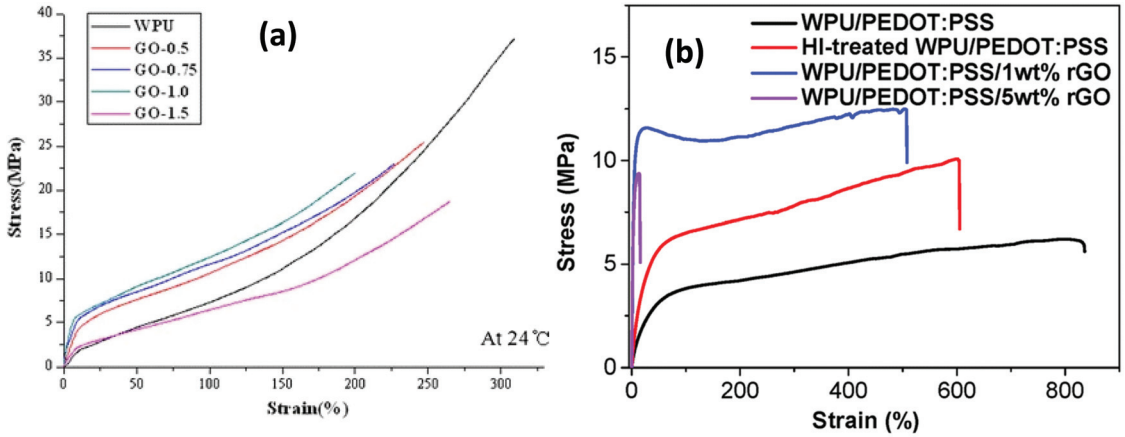

Fig. 9 Mechanical properties of Graphene/wPU composites, (a) GO/wPU. Reprinted with permission from ref. 238. Copyright 2013 Springer-Verlag. (b) rGO/wPU–PEDOT:PSS.[239]

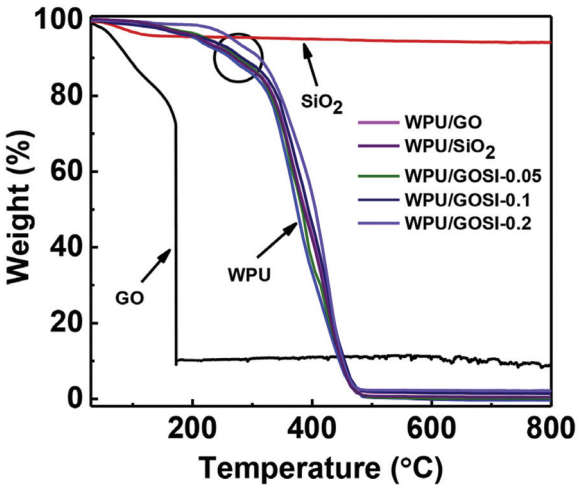

Fig. 10 Thermogravimetric analysis (TGA) of graphene-based PU composites, wPU/GOSI (GO–silica), wPU/GO and wPU/SiO_2 composites. Reprinted with permission from ref. 241. Copyright 2019 Elsevier.

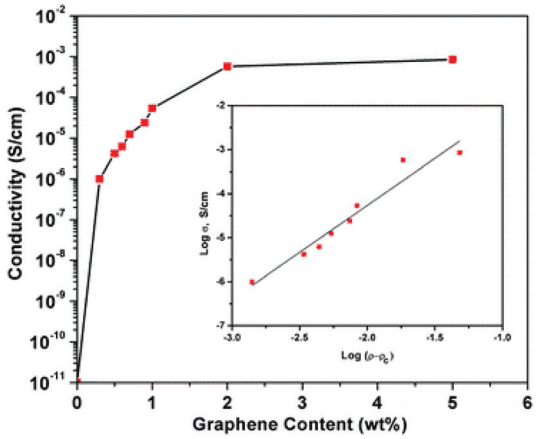

Fig. 11 Electrical conductivity (ϕ_c) of the graphene elastomer composite as a function of the % graphene loading (ρ): rGO/PU. Insert: log plot of ϕ_c against log ($\rho - \rho_c$), where ρ_c is the percolation threshold. Reprinted with permission from ref. 219. Copyright 2012 Royal Society of Chemistry.

WBE. Nevertheless, the mechanism of the electrical conductivity inducement of WBE with graphene-based materials remains largely unknown.

3.3. Structure–property relationship characterisation

Microscopy techniques, such as SEM and TEM, are notably employed for the structural and morphological characterisation of graphene/elastomer composites. Although other techniques, such as AFM and optical microscopy (OP-M), can also be utilised in graphene-composites analysis, they are however predominantly used in graphene materials analysis.

However, a majority of the available reports on G–WBEC employ SEM and TEM for the surface morphology characterisation of the composites. Tian *et al.* recently utilised SEM and TEM in dispersion analysis of rGO/wPU composites. The result obtained by Tian *et al.* (Fig. 12a–h) showed a well-dispersed graphene sheet structure for both GO (Fig. 12a) and nitrogen-functionalised rGO (Fig. 12b), unlike the smooth structured wPU (Fig. 12c) and the wrinkled rough surface structure observed for the rGO/wPU composite (Fig. 12d–g), which is attributable to well-dispersed graphene sheets within the elastomeric matrix.[260] Also, the TEM image in Fig. 12h is an indication of the continuous graphene network structure within the elastomeric matrix. Thus, it provides details about the reinforcement pattern of G–WBEC, which has a resultant effect on the property of the composite in terms of either mechanical, electrical or thermal characteristics. Similar reports, such as those on GO–silica/wPU,[241] functionalised-GNPs/wPU acrylate[261] and GO-microcapsules/wPU,[262] also utilised SEM and TEM for the surface structural and morphological analysis of the materials.

Additionally, an earlier report by Choi *et al.*[245] showed that OP-M can be utilised in the analysis of graphene/wPU composites. Nevertheless, obtaining detailed information from OP-M

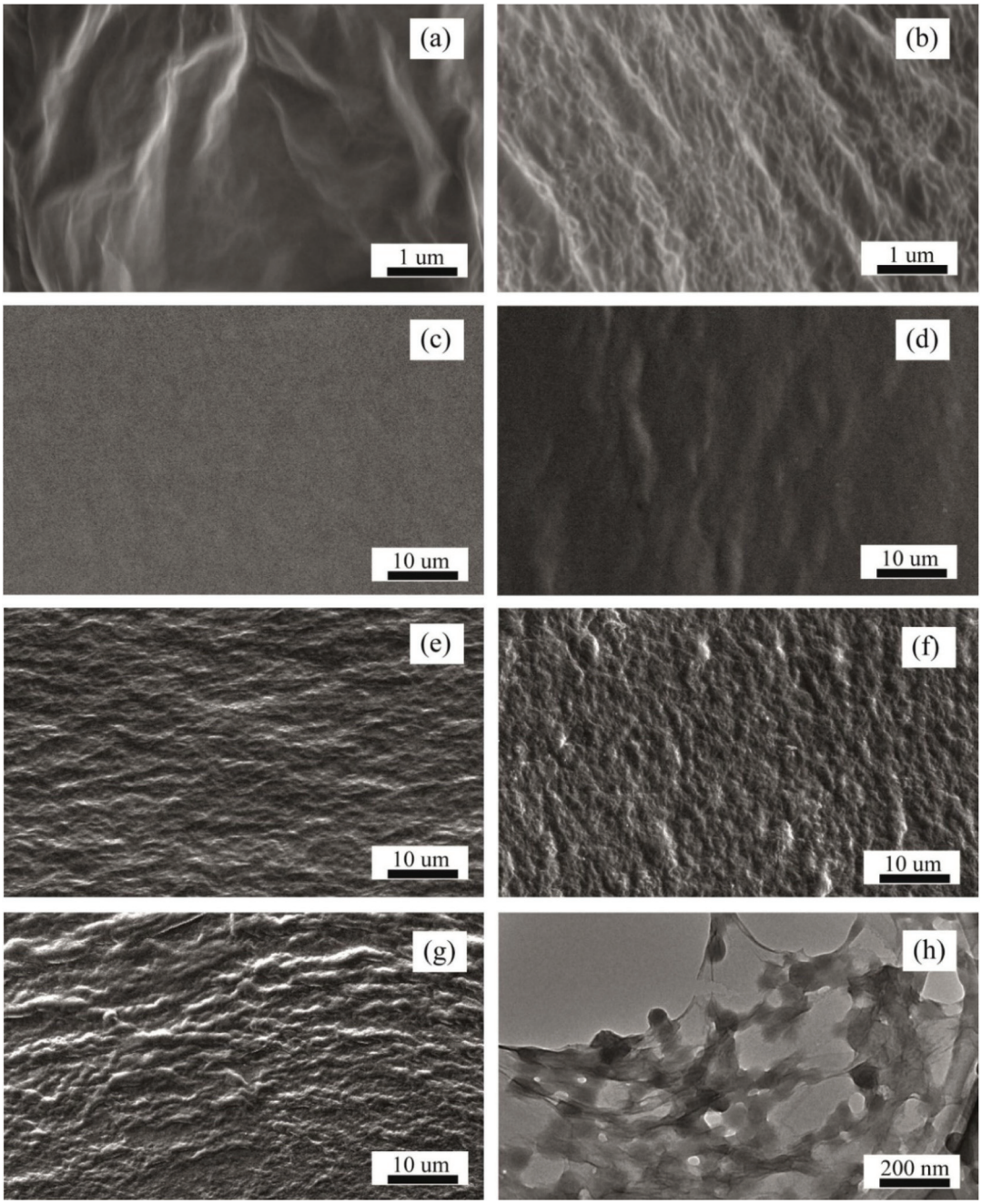

Fig. 12 SEM micrograph of (a) GO, (b) nitrogen-functionalised rGO (n-rGO), (c) pure wPU; and n-rGO/wPU composite at (d) 1 wt% loading, (e) 5 wt% loading, (f) 9 wt% loading, (g) 12 wt% loading; (h) TEM micrograph of the n-rGO/wPU composites at 5 wt% n-rGO loading. Reprinted with permission from ref. 260. Copyright 2017 Elsevier.

requires an expert-eye, as the results appear to lack detail and clarity. In 2016, Iliut *et al.*[218] employed AFM to study the structure and morphology of G–WBEC (Fig. 13). The authors noted poor dispersibility of the GO sheets within the wPU matrix, which is contrary to the strong rGO sheets interaction with the wPU matrix (Fig. 13e and f).

Furthermore, X-ray diffraction spectroscopy (XRD) can be employed to establish the rate of graphitic sheet exfoliation (whether the reinforcement is based on monolayer or multi-layer stacks) within the composite matrix, which also provides significant information about any defect presence within the elastomeric matrix structure. This is achieved through changes in the peak intensity, which gives an indication of the graphene sheet interplanar spacing (*d*-spacing). An earlier report by Raghu *et al.* showed that there tends to be sharp diffraction peak patterns in wPU, which tend to flatten upon graphene introduction (Fig. 14), as the nanofiller % loading tends to suppress the wPU hard segments.[249] Thus, this provides a

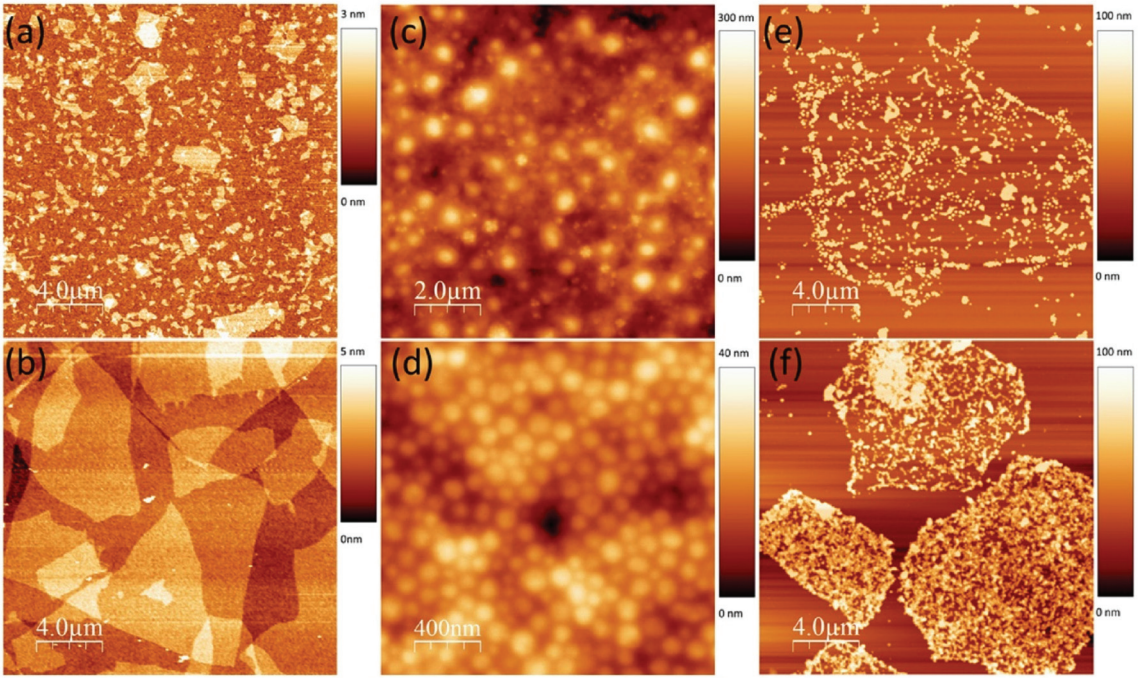

Fig. 13 AFM micrographs of: (a) small GO sheets, (b) large GO sheets, (c) pure natural rubber latex (d) pure wPU, (e) GO/wPU, and (f) rGO/wPU.[218]

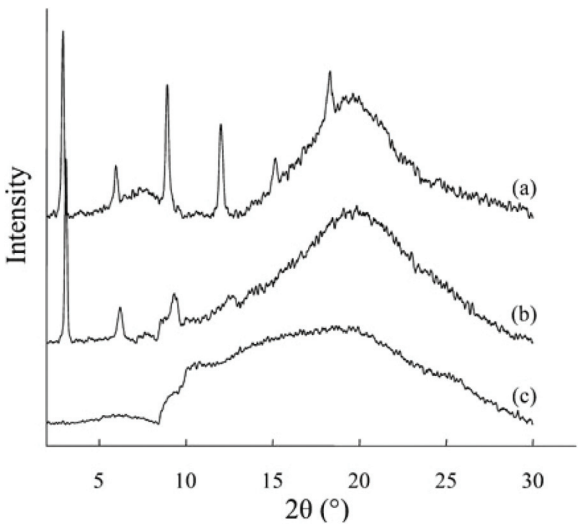

Fig. 14 XRD pattern of the graphene wPU composites: (a) wPU, (b) graphene/wPU (3 wt% loading), and (c) graphene/wPU (at 6 wt% loading). Reprinted with permission from ref. 249. Copyright 2008 Wiley-VCH Verlag GmbH & Co.

strong indication of the graphene dispersion within the elastomeric matrix, as well as a proper understanding of the composite property characteristics.

Besides XRD, another non-destructive analytical technique (such as Raman spectroscopy) is tauted as the most reliable structural characterisation tool for graphene-based nanocomposites due to its ability to assess the interface load transfer efficiency of graphene nanofiller sheets.[237] Thus, Raman seems to provide a greater understanding of the rate of filler dispersion within the elastomeric matrix, as recently demonstrated by Bernard *et al.*[222] The authors employed Raman to establish the uniformity of a homogenous dispersion of GO across various surface structural locations of a wPU composite, with the D and G bands maintaining close consistency in the wavenumber and peak intensity, as presented in Fig. 15.

4. Potential industrial applications of G–WBEC

The utilisation of WBE, such as NRL, wPU and wSi, cuts across various industrial sectors; for instance, building, textiles, and medical industries (Fig. 16), which tend to expand in the nearest future with the arrival of newer WBE formulations like wEPDM.

However, the introduction of graphene nanofillers with its attendant property enhancement features is currently attracting special attention. As graphene integration into WBE is expected to widen the WBE areas of application into high-performance and multifunctional engineering elastomers, that can be broadly employed in a wide range of sectors. Although there are no developed industrial products yet, G–WBEC can be employed in various areas of applications, such as multifunctional and non-functional coatings as highlighted in Fig. 17.

4.1. Aerospace

Employing G–WBEC in aircraft coatings can help induce smart features, like triggering the self-de-icing of the aircraft parts

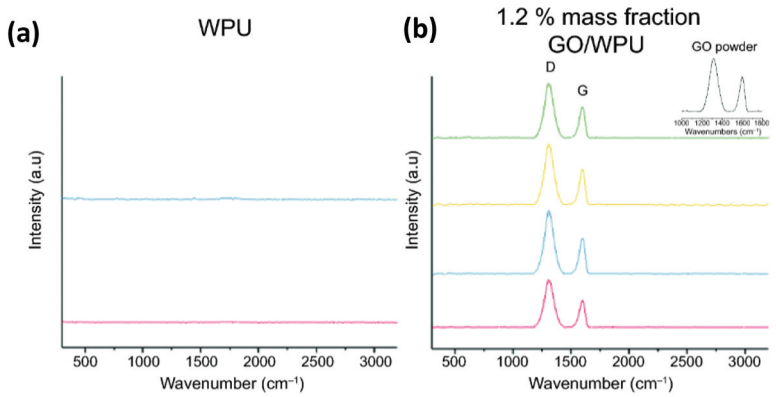

Fig. 15 Raman spectra of (a) wPU, (b) GO/wPU at 1.2% graphene loading, with D and G bands maintaining close consistency in the peak and wavenumber variation across various location points of the specimen. Reprinted with permission from ref. 222. Copyright 2019 American Coatings Association.

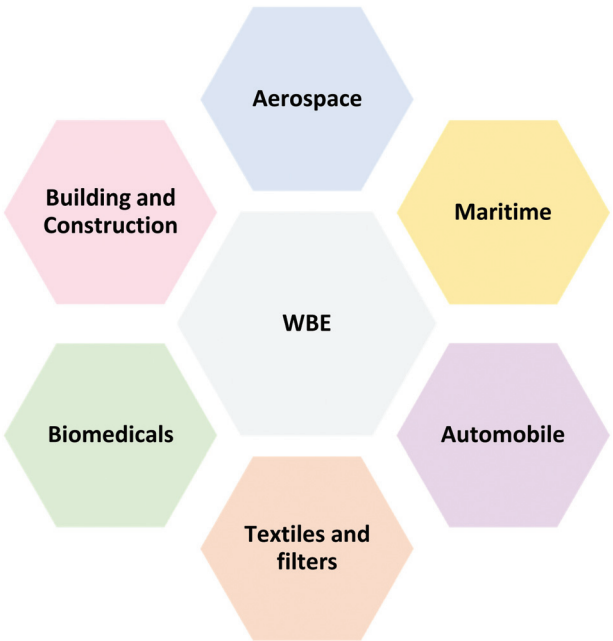

Fig. 16 WBE areas of industrial application.

under extreme low temperature conditions. This is achievable by utilising the electrical conductivity property inherent in graphene elastomeric composites. Also, the G–WBEC coating can help sustain the life-span of an aircraft under high temperature conditions (by taking advantage of the high thermal stability and conductivity of graphene), as well as offer anticorrosive properties to the metallic parts under corrosive environments.

G–WBEC coatings are also capable of offering strong electromagnetic interference (EMI) shielding in surveillance aircrafts (having achieved about 32 dB attenuation in the graphene–nanosheet/wPU composite at ~7.7 wt% graphene loading),[263] as well as offering lightweight gain and resultant lesser fuel consumption. In addition, G–WBEC can be employed in the production of enhanced and sustainable aircraft interior fixtures and fittings.

4.2. Maritime

G–WBEC is promising for maritime transport, as it can be utilised as antifouling and anticorrosion coatings[264,265] in marine vehicles, such as ships, yachts, boats, and submarines, with the possibility to offer multifunctional properties, such as the requirement for de-icing and EMI shielding,[263] as well as the functional interior decor of the marine vehicles like conductive screen coatings.

4.3. Automotive

The automobile industry is another major sector for G–WBEC applications in the areas of lightweight gain, smart interior fixtures, energy efficiency and unmanned (driverless) vehicles, with anti-scratch coating and de-icing capabilities. G–WBEC coatings can be employed in automobile engines and exteriors, as well as interior fixtures (Fig. 18), with great possibility for structural health monitoring in next generation automobiles.

4.4. Textiles and paper

Multifunctional G–WBEC are suitable materials for the next-generation of thermal wears[266] that can offer switching functions. Employing G–WBEC in textiles has the capability of providing camouflaging functions that can be utilised in high-tech military operations. Thus, G–WBEC offers the opportunity for strong and smart e-textile clothing,[267–270] leathers and papers that can be employed in body temperature/health monitoring. In addition, G-WBEC offers great prospect for the development of multifunctional fabric and paper filters for various applications, such as shoe fabric and sole coatings. A recent study by Shaun *et al.* on GO/wPU composite demonstrated that developing a wearable e-textile with strain sensing and high-elastic capability is achievable.[270] Also of note is the high level of washability that can be achieved in such G–WBEC textile materials.

4.5. Electronics

The conductive coatings of G–WBEC possess great potential for the production of the next-generation smart electronic

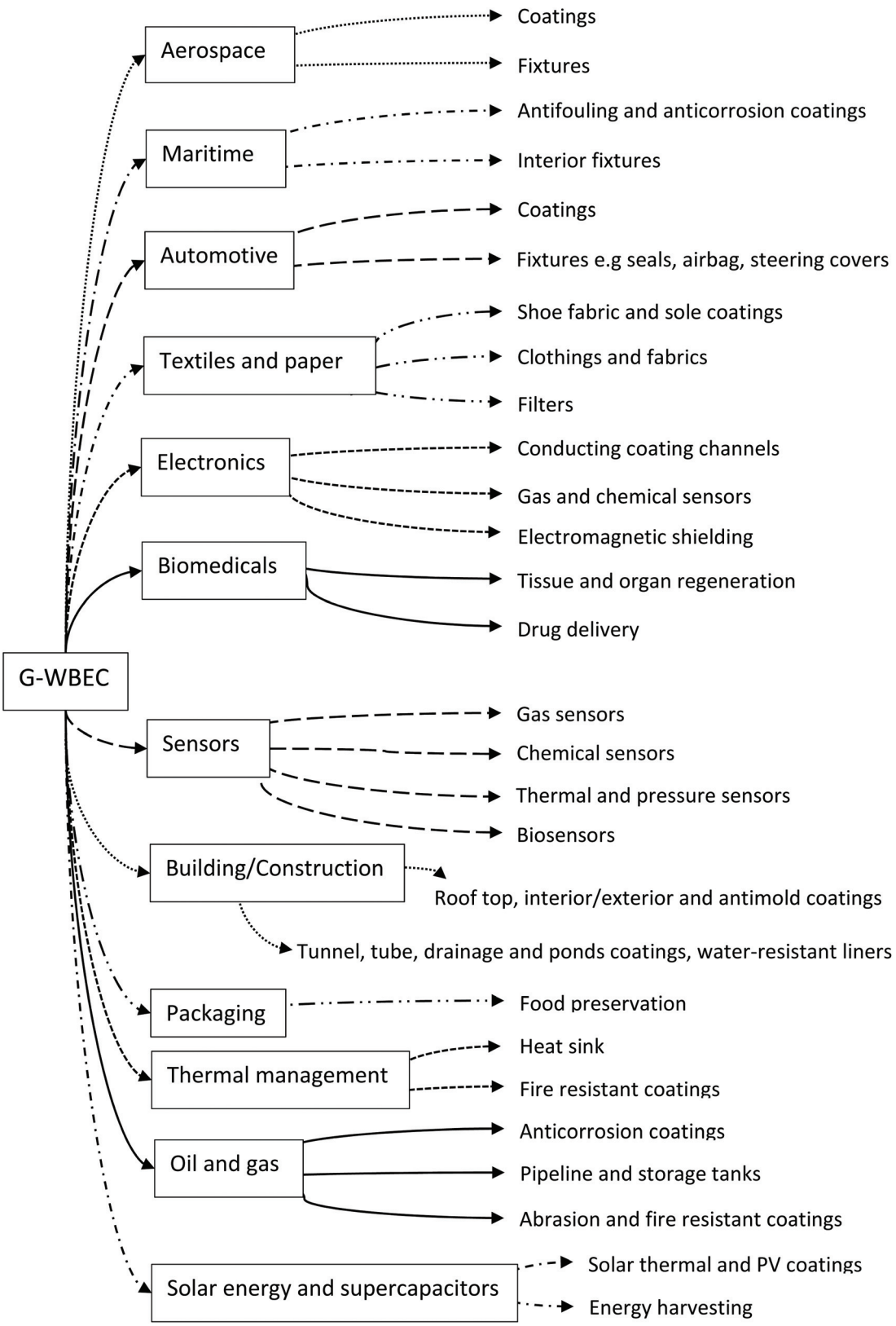

Fig. 17 Potential applications of G–WBEC.

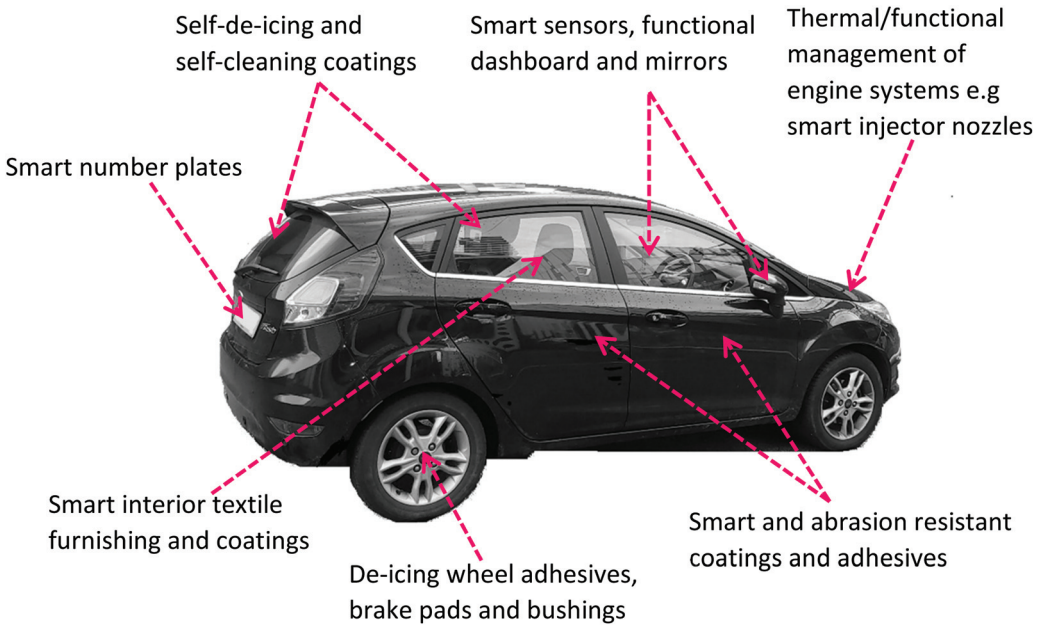

Fig. 18 Potential automotive applications of G–WBEC.

systems that can be employed in the development of foldable electronic devices, touch screens, nanopositioners and multifunctional integrated circuits. That are applicable in both consumer products, household gadgets, and high-tech electronic systems. Such studies are already being undertaken at the laboratory scale for application in sectors such as EMI shielding and transparent flexible heaters.[271–273]

4.6. Biomedicals

In biomedicals, G–WBEC can be readily employed in pharmaceuticals in the development of nanobots for on-target drug delivery and tumour therapy.[274] There is also the prospect of applying G–WBEC for tissue regenerations, for stronger and high throughput healing and repairs,[275] as well as the possibility for neurovascular regeneration, as recently demonstrated by Lee *et al.*[276] using the graphene/wPU composite.

4.7. Sensors

Several reports have demonstrated the ability of graphene to achieve remarkable sensitivity in several materials, as recently documented by Miao *et al.*[277] As such, G–WBEC possesses great prospect for the development of the next generation of gas-sensors, bio-sensors, chemical sensors, and pressure sensors, as well as EMI shielding systems,[15,263,270,278] with outstanding performance capabilities.

4.8. Building and construction

Due to the need to reduce the carbon footprint, as well as achieving high standard in building and construction industries, employing G–WBEC coatings can help reduce or perhaps eradicate the effect of combustion, as graphene possess excellent fire-resistant properties. Also, G–WBEC can offer stronger coatings in buildings, ponds, drainages, tunnels and tubes by serving as anti-corrosion,[265] antibacterial,[279] self-healing (anti-scratch) coatings,[248,280] as well as water-resistant liners[281] and fire-resistant[220] systems for possible cladding application. Additionally, there is great possibility of employing G–WBEC as multifunctional smart materials for wall interiors and exteriors, as well as roof tops, woods, concretes and paper coatings.

4.9. Packaging

G–WBEC can also be tailored for the development of breathable coatings, which can help forestall the massive occurrence of food wastage across the world, through safer preservation, by ensuring breathability, thus increase the lifespan of the food product as well as its nutritious content. Guan *et al.*[282] achieved a ~80% reduction in the oxygen permeability and <67% moisture absorption for a functionalised graphene–oxide/styrene–acrylic emulsion-based composite, which demonstrates its strong applicability for use in food packaging products. Also, integrating the antibacterial properties dominant in GO into WBE, such as wPU[283] and wIPR, will assist to ensure high level of food packaging safety in effect.

4.10. Thermal management

Due to the outstanding thermal properties of graphene, G–WBEC can offer a high degree of stability when employed as a heat sink,[284–286] and fire-resistant films, in systems such as electronic devices, aircraft and automobile engines, including industrial heating systems. For instance, graphene has been employed in developing fire resistant based-elastomeric systems, such as those based on graphene/wPU composites.[220,251]

4.11. Oil and gas

Elastomeric protective coatings are essential for the oil and gas industries in the areas of corrosion protection in seawater (off-shore environments), fire-resistant coatings, as well as abrasion and ozone resistant coatings.[287,288] WBEs, such as wEPDM, could offer remarkable protection in the development and repairs of oil and gas pipe installations, including steel riser pipes, offering stronger protection to splash zones, field joints, clamps and guides points.[287] Employing G–WBEC offers a possibility for the development of multifunctional coatings for the prospective real-time monitoring of pipelines, storage tanks, and other oil and gas installations, in both off-shore and on-shore environments.

4.12. Solar energy harvesting and supercapacitors

Although this area of graphene prospect is still not widely explored at the moment, a great opportunity exists by integrating graphene into WBE for the production of high-performing polymer solar cells.[289] Thus, recent reports indicate that as a highly transparent and conductive material, graphene is capable of serving as a hole transport layer[290] and a solar absorber[291] in photovoltaics and solar energy harvesting systems, as well as high-performing and flexible micro-supercapacitors with up to 200 W cm^{-3} power density.[292] Hence, this indicates that the G–WBEC coatings offer great prospect for the future of energy harvesting, solar thermal and photovoltaics industry.

5. Conclusions and outlook

In conclusion, this review provides a summary of the recent developments on graphene-based materials, G–WBEC production methods, its characterisation techniques, properties, and potential areas of application. Techniques, such as ball-milling, jet-cavitation, and electrochemical exfoliation, are observed to possess a strong potential for the facile high-throughput production of quality graphene.

Promising G–WBEC production technologies, such as emulsion mixing (blending), and *in situ* polymerisation systems like Pickering, micro-emulsion and mini-emulsion polymerisation, as well as ball-milling strategies were also reviewed in this study, providing details on the differences existing between the various pathways. Both techniques are observed to offer strong potential for the development of G–WBEC with outstanding mechanical, electrical and thermal properties. Hence, overcoming poor mechanical and thermal properties inherent in WBE enhances their potentials for deployment as high-performing multifunctional elastomeric engineering materials.

The emulsion mixing technique seems to be more facile with less time consumption compared to the *in situ* polymerisation process. The study also offers a critical review on the structure–property relationships of G–WBEC, analysing the impact of the graphene filler dispersion and filler–matrix interface on the composite material *via* techniques, such as Raman, XRD, and electron microscopy techniques. The analysis so far indicates that poor graphene dispersion, agglomeration and poor filler–matrix interface impact negatively on the final product (composite), as this results in a poor load transfer and poor percolated network within the elastomeric matrix, leading to a reduction in the mechanical properties and low electrical conductivity, as well as poor thermal stability and conductivity. Hence, to overcome these challenges, there is need for proper fine-tuning of the production processes and possible surface functionalisation of the graphene derivatives. The available results also indicate that achieving simultaneous improvement in the properties is not yet a possibility, thus more efforts are to be geared towards an application specific property, while compromising on other associated properties.

Furthermore, there is a need for the real-time analysis of G–WBEC properties during production, as there appears to be no available literature in this regard. The available data also suggest that NRL and wPU remain the most widely studied WBE, with wPU being the most formulated synthetic WBE. In addition, studies on wSi and wSBR are largely limited, while other WBE such as wEPDM remain unexplored. Also, the existence of graphene based wIPR composite formulations remain largely elusive, as there appears to be no significant literature on such composites. However, significant work exists on graphene/NRL based composites. The reason behind the under-utilisation of graphene in wIPR reinforcement remain yet to be understood, hence an indication that there exists a vacuum yet to be filled in this area of research. Development of graphene/wIPR composites will possibly lead to the production of more durable and enhanced rubber composites, contrary to what is currently obtainable with NRL. Being that IPR chemical composition can easily be modified and tailored to particular characteristics unlike NRL.

With the continual paradigm shift towards utilisation of WBE due to their eco-friendly nature, developing G–WBEC offers a reliable solution towards offsetting the poor mechanical and thermal properties inherent in pristine WBE. For instance, graphene has been shown to improve the tensile strength and elastic modulus of WBE from ~7–706%, and ~10–1245%, respectively, as well as an improvement in the thermal stability with an increase of ~9.1–44.48 °C increase in the thermal decomposition temperature achieved. In addition, the study has shown that an increase of up to ~38–483% in thermal conductivity, as well as ~3.54 × 10^{-12}–5.7 S cm^{-1} increase in the electrical conductivity of WBE have been achieved through graphene materials incorporation, which are critical for the technical and multifunctional applications of this set of elastomeric materials. Nevertheless, it is worth noting that graphene addition does not actually lead to a simultaneous improvement in the properties, nor give the same level of enhancement, since some properties might get worse. For instance, the available results indicate that there is a greater tendency for a gradual drop in elongation to break with an increase in the graphene loading, and there might also be unsatisfactory drop in tensile strength. Hence, there is a need for a proper optimisation of each kind of G–WBEC formu-

lation, which is largely dependent on the intended specific application.

G–WBEC exhibits cumulative properties for potential applications in both general purpose and high-tech multifunctional engineering systems, in sectors such as aerospace, maritime, automotive, textiles and paper, electronics, biomedicals, sensors, building and construction, packaging, thermal management, oil and gas, solar energy harvesting, as well as supercapacitors. Finally, there is a need for clear synergy between academia and industry with regards to graphene and WBE formulation and production, in order to effectively harness the enormous commercial potentials inherent in G–WBEC.

Conflicts of interest

There are no conflicts to declare.

Acknowledgements

CNN acknowledges sponsorship from the Petroleum Technology Development Fund (PTDF), Nigeria.

References

1 L. W. McKeen, Elastomers and Rubbers, in *The Effect of UV Light and Weather on Plastics and Elastomers*, Elsevier, 4th edn, 2019, pp. 279–359.
2 A. Bahadori, Corrosion in Pipelines and Piping Systems, in *Oil and Gas Pipelines and Piping Systems*, Elsevier, 2017, pp. 395–481.
3 L. Valentini and M. A. Lopez-Manchado, Rubber nanocomposites for extreme environments: Critics and counterintuitive solutions, *Front. Mater.*, 2018, **5**, 49, DOI: 10.3389/fmats.2018.00049.
4 H. Honarkar, Waterborne polyurethanes: A review, *J. Dispersion Sci. Technol.*, 2018, **39**(4), 507–516, DOI: 10.1080/01932691.2017.1327818.
5 W. Lei, X. Zhou, C. Fang, Y. Song and Y. Li, Eco-friendly waterborne polyurethane reinforced with cellulose nanocrystal from office waste paper by two different methods, *Carbohydr. Polym.*, 2019, **209**, 299–309, DOI: 10.1016/j.carbpol.2019.01.013.
6 D. Wu, F. Qiu, H. Xu, J. Zhang and D. Yang, Preparation, Characterization, and Properties of Environmentally Friendly Waterborne Poly(urethane acrylate)/Silica Hybrids, *J. Appl. Polym. Sci.*, 2010, **119**, 1683–1695, DOI: 10.1002/app.
7 T. Easton and S. Poultney, Waterborne silicone-organic hybrid coatings for exterior applications, *J. Coat. Technol. Res.*, 2007, **4**(2), 187–190, DOI: 10.1007/s11998-007-9018-z.
8 W. M. Cole, G. G. A. Bohm, W. Tomaszewski and Y. Huang, *US Pat.*, 8815965, 2014.
9 E. Yip and P. Cacioli, The manufacture of gloves from natural rubber latex, *J. Allergy Clin. Immunol.*, 2002, **110**(2), S3–S14, DOI: 10.1067/mai.2002.124499.
10 N. Hassim, M. R. Ahmad, W. Y. W. Ahmad, A. Samsuri and M. H. M. Yahya, Puncture resistance of natural rubber latex unidirectional coated fabrics, *J. Ind. Text.*, 2011, **42**(2), 118–131, DOI: 10.1177/1528083711429144.
11 J. Kodemura, S. Aihara and Y. Satoh, *US Pat.*, 0062873, 2020.
12 D. M. Lucas, S. Amarasekera, D. Narasimhan and A. A. L. Kung, *US Pat.*, 9725539, 2017.
13 N. Calderon, K. F. Castner, H. A. Colvin and J. Joel Muse, *US Pat.*, 6066705, 2000.
14 F. W. Stavely, Coral Rubber—A Cis-1,4-Polyisoprene, *Rubber Chem. Technol.*, 1956, **29**(3), 673–686, DOI: 10.5254/1.3542582.
15 Y. Ahmadi and S. Ahmad, Recent Progress in the Synthesis and Property Enhancement of Waterborne Polyurethane Nanocomposites: Promising and Versatile Macromolecules for Advanced Applications, *Polym. Rev.*, 2020, **60**(2), 226–266, DOI: 10.1080/15583724.2019.1673403.
16 F. Wang and J. Mao, Nacre-like graphene oxide/waterborne styrene butadiene rubber composite and its reusable anticorrosion behavior on Al-2024, *Prog. Org. Coat.*, 2019, **132**, 191–200, DOI: 10.1016/j.porgcoat.2019.03.048.
17 J. S. Kim, S. Hong, D. W. Park and S. E. Shim, Waterborne graphene-derived conductive SBR prepared by latex heterocoagulation, *Macromol. Res.*, 2010, **18**(6), 558–565, DOI: 10.1007/s13233-010-0603-0.
18 A. Santamaria-Echart, L. Ugarte, C. García-Astrain, A. Arbelaiz, M. A. Corcuera and A. Eceiza, Cellulose nanocrystals reinforced environmentally-friendly waterborne polyurethane nanocomposites, *Carbohydr. Polym.*, 2016, **151**, 1203–1209, DOI: 10.1016/j.carbpol.2016.06.069.
19 M. Serkis, M. Špírková, J. Hodan and J. Kredatusová, Nanocomposites made from thermoplastic waterborne polyurethane and colloidal silica. The influence of nanosilica type and amount on the functional properties, *Prog. Org. Coat.*, 2016, **101**, 342–349, DOI: 10.1016/j.porgcoat.2016.07.021.
20 C. Lee, X. Wei, J. W. Kysar and J. Hone, Measurement of the elastic properties and intrinsic strength of monolayer graphene, *Science*, 2008, **321**(5887), 385–388, DOI: 10.1126/science.1157996.
21 T. Cui, *et al*. Fatigue of graphene, *Nat. Mater.*, 2020, **19**, 405–411, DOI: 10.1038/s41563-019-0586-y.
22 A. A. Balandin, *et al*. Superior Thermal Conductivity of Single-Layer Graphene, *Nano Lett.*, 2008, **8**(3), 902–907, DOI: 10.1021/nl0731872.
23 S. V. Morozov, *et al*. Giant intrinsic carrier mobilities in graphene and its bilayer, *Phys. Rev. Lett.*, 2008, **100**, 016602, DOI: 10.1103/PhysRevLett.100.016602.
24 K. I. Bolotin, *et al*. Ultrahigh electron mobility in suspended graphene, *Solid State Commun.*, 2008, **146**(9–10), 351–355, DOI: 10.1016/j.ssc.2008.02.024.

25 X. Du, I. Skachko, A. Barker and E. Y. Andrei, Approaching ballistic transport in suspended graphene, *Nat. Nanotechnol.*, 2008, **3**, 491–495, DOI: 10.1038/nnano.2008.199.
26 K. K. Sadasivuni, D. Ponnamma, S. Thomas and Y. Grohens, Evolution from graphite to graphene elastomer composites, *Prog. Polym. Sci.*, 2014, **39**(4), 749–780, DOI: 10.1016/j.progpolymsci.2013.08.003.
27 B. Mensah, K. C. Gupta, H. Kim, W. Wang, K. U. Jeong and C. Nah, Graphene-reinforced elastomeric nanocomposites: A review, *Polym. Test.*, 2018, **68**, 160–184, DOI: 10.1016/j.polymertesting.2018.04.009.
28 D. G. Papageorgiou, I. A. Kinloch and R. J. Young, Graphene/elastomer nanocomposites, *Carbon*, 2015, **95**, 460–484, DOI: 10.1016/j.carbon.2015.08.055.
29 S. Araby, Q. Meng, L. Zhang, I. Zaman, P. Majewski and J. Ma, Elastomeric composites based on carbon nanomaterials, *Nanotechnology*, 2015, **26**(11), 112001, DOI: 10.1088/0957-4484/26/11/112001.
30 K. S. Novoselov, *et al*. Electric field in atomically thin carbon films, *Science*, 2004, **306**(5696), 666–669, DOI: 10.1126/science.1102896.
31 S. Stankovich, *et al*. Graphene-based composite materials, *Nature*, 2006, **442**, 282–286, DOI: 10.1038/nature04969.
32 J. R. Potts, D. R. Dreyer, C. W. Bielawski and R. S. Ruoff, Graphene-based polymer nanocomposites, *Polymer*, 2011, **52**, 5–25.
33 A. K. Geim and K. S. Novoselov, The rise of graphene, *Nat. Mater.*, 2007, **6**, 183–191, DOI: 10.1038/nnano.2010.224.
34 A. Vijayaraghavan, Graphene – Properties and Characterization, in *Springer Handbook of Nanomaterials*, ed. R. Vajtai, Springer-Verlag, Berlin Heidelberg, 2013, pp. 39–82.
35 A. Vijayaraghavan and M. Iliut, Graphene, in *Springer Handbook of Nanotechnology*, ed. B. Bhushan, Springer-Verlag, Berlin Heidelberg, 2017, pp. 363–391.
36 S. J. Woltornist, A. J. Oyer, J. M. Y. Carrillo, A. V. Dobrynin and D. H. Adamson, Conductive thin films of pristine graphene by solvent interface trapping, *ACS Nano*, 2013, **7**(8), 7062–7066, DOI: 10.1021/nn402371c.
37 L. H. Liu, M. M. Lerner and M. Yan, Derivitization of pristine graphene with well-defined chemical functionalities, *Nano Lett.*, 2010, **10**(9), 3754–3756, DOI: 10.1021/nl1024744.
38 A. Bianco, *et al*. All in the graphene family - A recommended nomenclature for two-dimensional carbon materials, *Carbon*, 2013, **65**, 1–6, DOI: 10.1016/j.carbon.2013.08.038.
39 K. Kim, *et al*. High-temperature stability of suspended single-layer graphene, *Phys. Status Solidi RRL*, 2010, **4**(11), 302–304, DOI: 10.1002/pssr.201000244.
40 F. Liu, P. Ming and J. Li, Ab initio calculation of ideal strength and phonon instability of graphene under tension, *Phys. Rev. B: Condens. Matter Mater. Phys.*, 2007, **76**, 064120, DOI: 10.1103/PhysRevB.76.064120.
41 O. L. Blakslee, D. G. Proctor, E. J. Seldin, G. B. Spence and T. Weng, Elastic constants of compression-annealed pyrolytic graphite, *J. Appl. Phys.*, 1970, **41**(8), 3373–3382, DOI: 10.1063/1.1659428.
42 D. Sánchez-Portal, E. Artacho, J. M. Soler, A. Rubio and P. Ordejón, Ab initio structural, elastic, and vibrational properties of carbon nanotubes, *Phys. Rev. B*, 1999, **59**(19), 12678, DOI: 10.1103/PhysRevB.59.12678.
43 A. A. Balandin, Thermal properties of graphene and nanostructured carbon materials, *Nat. Mater.*, 2011, **10**, 569–581, DOI: 10.1038/nmat3064.
44 D. L. Nika, S. Ghosh, E. P. Pokatilov and A. A. Balandin, Lattice thermal conductivity of graphene flakes: Comparison with bulk graphite, *Appl. Phys. Lett.*, 2009, **94**, 203103, DOI: 10.1063/1.3136860.
45 D. L. Nika, E. P. Pokatilov, A. S. Askerov and A. A. Balandin, Phonon thermal conduction in graphene: Role of Umklapp and edge roughness scattering, *Phys. Rev. B: Condens. Matter Mater. Phys.*, 2009, **79**, 155413, DOI: 10.1103/PhysRevB.79.155413.
46 W. J. Evans, L. Hu and P. Keblinski, Thermal conductivity of graphene ribbons from equilibrium molecular dynamics: Effect of ribbon width, edge roughness, and hydrogen termination, *Appl. Phys. Lett.*, 2010, **96**(20), 203112, DOI: 10.1063/1.3435465.
47 Z. Wang, *et al*. Thermal Transport in Suspended and Supported Few-Layer Graphene, *Nano Lett.*, 2011, **11**, 113–118, DOI: 10.1021/nl102923q.
48 X. Xu, *et al*, Phonon Transport in Suspended Single Layer Graphene, *Preprint at https://arxiv.org/abs/1012.2937*, 2010.
49 M. T. Pettes, I. Jo, Z. Yao and L. Shi, Influence of polymeric residue on the thermal conductivity of suspended bilayer graphene, *Nano Lett.*, 2011, **11**(3), 1195–1200, DOI: 10.1021/nl104156y.
50 A. A. Balandin, S. Ghosh, D. L. Nika and E. P. Pokatilov, Thermal conduction in suspended graphene layers, *Fullerenes, Nanotubes, Carbon Nanostruct.*, 2010, **18**(4–6), 474–486, DOI: 10.1080/1536383X.2010.487785.
51 Y. Y. Zhang, Q. X. Pei, Y. Cheng, Y. W. Zhang and X. Zhang, Thermal conductivity of penta-graphene: The role of chemical functionalization, *Comput. Mater. Sci.*, 2017, **137**, 195–200, DOI: 10.1016/j.commatsci.2017.05.042.
52 D. L. Nika and A. A. Balandin, Two-dimensional phonon transport in graphene, *J. Phys.: Condens. Matter*, 2012, **24**, 233203, DOI: 10.1088/0953-8984/24/23/233203.
53 M. M. Sadeghi, M. T. Pettes and L. Shi, Thermal transport in graphene, *Solid State Commun.*, 2012, **152**(15), 1321–1330, DOI: 10.1016/j.ssc.2012.04.022.
54 P. N. Nirmalraj, T. Lutz, S. Kumar, G. S. Duesberg and J. J. Boland, Nanoscale mapping of electrical resistivity and connectivity in graphene strips and networks, *Nano Lett.*, 2011, **11**(1), 16–22, DOI: 10.1021/nl101469d.
55 A. I. Romanenko, O. B. Anikeeva, V. L. Kuznetsov, A. N. Obrastsov, A. P. Volkov and A. V. Garshev, Quasi-two-dimensional conductivity and magnetoconductivity of graphite-like nanosize crystallites, *Solid State Commun.*, 2006, **137**(11), 625–629, DOI: 10.1016/j.ssc.2006.01.003.

56 X. Y. Fang, X. X. Yu, H. M. Zheng, H. B. Jin, L. Wang and M. S. Cao, Temperature- and thickness-dependent electrical conductivity of few-layer graphene and graphene nanosheets, *Phys. Lett. A*, 2015, **379**(37), 2245–2251, DOI: 10.1016/j.physleta.2015.06.063.

57 B. Marinho, M. Ghislandi, E. Tkalya, C. E. Koning and G. de With, Electrical conductivity of compacts of graphene, multi-wall carbon nanotubes, carbon black, and graphite powder, *Powder Technol.*, 2012, **221**, 351–358, DOI: 10.1016/j.powtec.2012.01.024.

58 K. Kanghyun, J. P. Hyung, B. C. Woo, J. K. Kook, T. K. Gyu and S. Y. Wan, Electric property evolution of structurally defected multilayer grapheme, *Nano Lett.*, 2008, **8**(10), 3092–3096, DOI: 10.1021/nl8010337.

59 M. E. Uddin, T. Kuila, G. C. Nayak, N. H. Kim, B. C. Ku and J. H. Lee, Effects of various surfactants on the dispersion stability and electrical conductivity of surface modified graphene, *J. Alloys Compd.*, 2013, **562**, 134–142, DOI: 10.1016/j.jallcom.2013.01.127.

60 T. Ma, *et al*. Tailoring the thermal and electrical transport properties of graphene films by grain size engineering, *Nat. Commun.*, 2017, **8**, 14486, DOI: 10.1038/ncomms14486.

61 T. P. Raine, O. M. Istrate, B. E. King, B. Craster, I. A. Kinloch and P. M. Budd, Graphene/Polyamide Laminates for Supercritical CO_2 and H2S Barrier Applications: An Approach toward Permeation Shutdown, *Adv. Mater. Interfaces*, 2018, **5**(15), 1800304, DOI: 10.1002/admi.201800304.

62 L. J. van Rooyen, H. Bissett, M. C. Khoathane and J. Karger-Kocsis, Gas barrier properties of oxyfluorinated graphene filled polytetrafluoroethylene nanocomposites, *Carbon*, 2016, **109**, 30–39, DOI: 10.1016/j.carbon.2016.07.063.

63 D. Pierleoni, *et al*. Graphene-based coatings on polymer films for gas barrier applications, *Carbon*, 2016, **96**, 503–512, DOI: 10.1016/j.carbon.2015.09.090.

64 S. Nam, Y. J. Jeong, C. E. Park and J. Jang, Enhanced gas barrier properties of graphene-TiO2 nanocomposites on plastic substrates assisted by UV photoreduction of graphene oxide, *Org. Electron.*, 2017, **48**, 323–329, DOI: 10.1016/j.orgel.2017.06.032.

65 H. Ha, J. Park, K. R. Ha, B. D. Freeman and C. J. Ellison, Synthesis and gas permeability of highly elastic poly(dimethylsiloxane)/graphene oxide composite elastomers using telechelic polymers, *Polymer*, 2016, **93**, 53–60, DOI: 10.1016/j.polymer.2016.04.016.

66 H. Liu, C. Liu, S. Peng, B. Pan and C. Lu, Effect of polyethyleneimine modified graphene on the mechanical and water vapor barrier properties of methyl cellulose composite films, *Carbohydr. Polym.*, 2018, **182**, 52–60, DOI: 10.1016/j.carbpol.2017.11.008.

67 S. Hocker, N. Hudson-Smith, H. C. Schniepp and D. E. Kranbuehl, Enhancing polyimide's water barrier properties through addition of functionalized graphene oxide, *Polymer*, 2016, **93**, 23–29, DOI: 10.1016/j.polymer.2016.04.008.

68 K. Honaker, F. Vautard and L. T. Drzal, Investigating the mechanical and barrier properties to oxygen and fuel of high density polyethylene–graphene nanoplatelet composites, *Mater. Sci. Eng., B*, 2017, **216**, 23–30, DOI: 10.1016/j.mseb.2016.10.005.

69 H. Mohammed, *et al*. Antimicrobial Mechanisms and Effectiveness of Graphene and Graphene-Functionalized Biomaterials. A Scope Review, *Front. Bioeng. Biotechnol.*, 2020, **8**, 465, DOI: 10.3389/fbioe.2020.00465.

70 A. P. Johnson, H. V. Gangadharappa and K. Pramod, Graphene nanoribbons: A promising nanomaterial for biomedical applications, *J. Controlled Release*, 2020, **325**, 141–162, DOI: 10.1016/j.jconrel.2020.06.034.

71 S. Song, *et al*. Biomedical application of graphene: From drug delivery, tumor therapy, to theranostics, *Colloids Surf., B*, 2020, **185**, 110596, DOI: 10.1016/j.colsurfb.2019.110596.

72 V. Georgakilas, *et al*. Noncovalent Functionalization of Graphene and Graphene Oxide for Energy Materials, Biosensing, Catalytic, and Biomedical Applications, *Chem. Rev.*, 2016, **116**(9), 5464–5519, DOI: 10.1021/acs.chemrev.5b00620.

73 P. Orsu and A. Koyyada, Recent progresses and challenges in graphene based nano materials for advanced therapeutical applications: a comprehensive review, *Mater. Today Commun.*, 2020, **22**, 100823, DOI: 10.1016/j.mtcomm.2019.100823.

74 Z. Ding, Z. Zhang, H. Ma and Y. Chen, In vitro hemocompatibility and toxic mechanism of graphene oxide on human peripheral blood T Lymphocytes and serum albumin, *ACS Appl. Mater. Interfaces*, 2014, **6**(22), 19797–19807, DOI: 10.1021/am505084s.

75 V. Palmieri, *et al*. Bacteria Meet Graphene: Modulation of Graphene Oxide Nanosheet Interaction with Human Pathogens for Effective Antimicrobial Therapy, *ACS Biomater. Sci. Eng.*, 2017, **3**(4), 619–627, DOI: 10.1021/acsbiomaterials.6b00812.

76 V. Palmieri, G. Perini, M. De Spirito and M. Papi, Graphene oxide touches blood: In vivo interactions of biocoronated 2D materials, *Nanoscale Horiz.*, 2019, **4**, 273–290, DOI: 10.1039/c8nh00318a.

77 B. F. M. Ribeiro, M. M. Souza, D. S. Fernandes, D. R. do Carmo and G. M. Machado-Santelli, Graphene oxide-based nanomaterial interaction with human breast cancer cells, *J. Biomed. Mater. Res., Part A*, 2020, **108**(4), 863–870, DOI: 10.1002/jbm.a.36864.

78 J. J. Castillo, W. E. Svendsen, N. Rozlosnik, P. Escobar, F. Martínez and J. Castillo-León, Detection of cancer cells using a peptide nanotube-folic acid modified graphene electrode, *Analyst*, 2013, **138**(4), 1026–1031, DOI: 10.1039/c2an36121c.

79 C. T. Laurencin and L. Daneshmandi, Graphene for regenerative engineering, *Int. J. Ceram. Eng. Sci.*, 2020, **2**(3), 140–143, DOI: 10.1002/ces2.10045.

80 N. Chauhan, T. Maekawa and D. N. S. Kumar, Graphene based biosensors - Accelerating medical diagnostics to

new-dimensions, *J. Mater. Res.*, 2017, **32**(15), 2860–2882, DOI: 10.1557/jmr.2017.91.

81 P. Hampitak, *et al*. Protein interactions and conformations on graphene-based materials mapped using quartz-crystal microbalance with dissipation monitoring (QCM-D), *Carbon*, 2020, **165**, 317–327, DOI: 10.1016/j.carbon.2020.04.093.

82 X. Zou, L. Zhang, Z. Wang and Y. Luo, Mechanisms of the Antimicrobial Activities of Graphene Materials, *J. Am. Chem. Soc.*, 2016, **138**(7), 2064–2077, DOI: 10.1021/jacs.5b11411.

83 Y. Tu, *et al*. Destructive extraction of phospholipids from Escherichia coli membranes by graphene nanosheets, *Nat. Nanotechnol.*, 2013, **8**, 594–601, DOI: 10.1038/nnano.2013.125.

84 A. Sharma, *et al*. Structural, electronic structure and antibacterial properties of graphene-oxide nano-sheets, *Chem. Phys. Lett.*, 2018, **698**, 85–92, DOI: 10.1016/j.cplett.2018.03.010.

85 W. Hu, *et al*. Graphene-based antibacterial paper, *ACS Nano*, 2010, **4**(7), 4317–4323, DOI: 10.1021/nn101097v.

86 H. M. Hegab, A. Elmekawy, L. Zou, D. Mulcahy, C. P. Saint and M. Ginic-Markovic, The controversial antibacterial activity of graphene-based materials, *Carbon*, 2016, **105**, 362–376, DOI: 10.1016/j.carbon.2016.04.046.

87 F. Lebre, *et al*. Pristine graphene induces innate immune training, *Nanoscale*, 2020, **12**(20), 11192–11200, DOI: 10.1039/c9nr09661b.

88 R. Sharma, J. H. Baik, C. J. Perera and M. S. Strano, Anomalously large reactivity of single graphene layers and edges toward electron transfer chemistries, *Nano Lett.*, 2010, **10**(2), 398–405, DOI: 10.1021/nl902741x.

89 H. Liu, S. Ryu, Z. Chen, M. L. Steigerwald, C. Nuckolls and L. E. Brus, Photochemical reactivity of graphene, *J. Am. Chem. Soc.*, 2009, **131**(47), 17099–17101, DOI: 10.1021/ja9043906.

90 C. E. Hamilton, J. R. Lomeda, Z. Sun, J. M. Tour and A. R. Barron, High-yield organic dispersions of unfunctionalized graphene, *Nano Lett.*, 2009, **9**(10), 3460–3462, DOI: 10.1021/nl9016623.

91 C. E. Hamilton, J. R. Lomeda, Z. Sun, J. M. Tour and A. R. Barron, Radical addition of perfluorinated alkyl iodides to multi-layered graphene and single-walled carbon nanotubes, *Nano Res.*, 2010, **3**, 138–145, DOI: 10.1007/s12274-010-1007-3.

92 L. Song, L. Ci, W. Gao and P. M. Ajayan, Transfer Printing of Graphene Using Gold Film, *ACS Nano*, 2009, **3**(6), 1353–1356, DOI: 10.1021/nn9003082.

93 R. Sharma, J. H. Baik, C. J. Perera and M. S. Strano, Anomalously large reactivity of single graphene layers and edges toward electron transfer chemistries, *Nano Lett.*, 2010, **10**(2), 398–405, DOI: 10.1021/nl902741x.

94 J. Park and M. Yan, Covalent functionalization of graphene with reactive intermediates, *Acc. Chem. Res.*, 2013, **46**(1), 181–189, DOI: 10.1021/ar300172h.

95 D. Chen, H. Feng and J. Li, Graphene oxide: Preparation, functionalization, and electrochemical applications, *Chem. Rev.*, 2012, **112**(11), 6027–6053, DOI: 10.1021/cr300115g.

96 L. Rodríguez-Pérez, M. Á. Herranz and N. Martín, The chemistry of pristine graphene, *Chem. Commun.*, 2013, **49**(36), 3721–3735, DOI: 10.1039/c3cc38950b.

97 V. Georgakilas, *et al*. Functionalization of graphene: Covalent and non-covalent approaches, derivatives and applications, *Chem. Rev.*, 2012, **112**(11), 6156–6214, DOI: 10.1021/cr3000412.

98 R. Sharma, N. Nair and M. S. Strano, Structure–Reactivity Relationships for Graphene Nanoribbons, *J. Phys. Chem. C*, 2009, **113**(33), 14771–14777, DOI: 10.1021/jp904814h.

99 D. G. Papageorgiou, I. A. Kinloch and R. J. Young, Mechanical properties of graphene and graphene-based nanocomposites, *Prog. Mater. Sci.*, 2017, **90**, 75–127, DOI: 10.1016/j.pmatsci.2017.07.004.

100 F. Bonaccorso, A. Lombardo, T. Hasan, Z. Sun, L. Colombo and A. C. Ferrari, Production and processing of graphene and 2d crystals, *Mater. Today*, 2012, **15**(12), 564–589, DOI: 10.1016/S1369-7021(13)70014-2.

101 W. Kundhikanjana, K. Lai, H. Wang, H. Dai, M. A. Kelly and Z.-X. Shen, Hierarchy of Electronic Properties of Chemically Derived and Pristine Graphene Probed by Microwave Imaging, *Nano Lett.*, 2009, **9**(11), 3762–3765, DOI: 10.1021/nl901949z.

102 J. P. Rourke, *et al*. The real graphene oxide revealed: Stripping the oxidative debris from the graphene-like sheets, *Angew. Chem., Int. Ed.*, 2011, **50**(14), 3173–3177, DOI: 10.1002/anie.201007520.

103 K. K. H. De Silva, H. H. Huang and M. Yoshimura, Progress of reduction of graphene oxide by ascorbic acid, *Appl. Surf. Sci.*, 2018, **447**, 338–346, DOI: 10.1016/j.apsusc.2018.03.243.

104 B. Z. Jang and A. Zhamu, Processing of nanographene platelets (NGPs) and NGP nanocomposites: A review, *J. Mater. Sci.*, 2008, **43**, 5092–5101, DOI: 10.1007/s10853-008-2755-2.

105 P. Wick, *et al*. Classification framework for graphene-based materials, *Angew. Chem., Int. Ed.*, 2014, **53**(30), 7714–7718, DOI: 10.1002/anie.201403335.

106 R. Ye and J. M. Tour, Graphene at Fifteen, *ACS Nano*, 2019, **13**(10), 10872–10878, DOI: 10.1021/acsnano.9b06778.

107 P. Kumar, U. N. Maiti, K. E. Lee and S. O. Kim, Rheological properties of graphene oxide liquid crystal, *Carbon*, 2014, **80**, 453–461, DOI: 10.1016/j.carbon.2014.08.085.

108 A. Pazat, C. Barrès, F. Bruno, C. Janin and E. Beyou, Preparation and Properties of Elastomer Composites Containing 'Graphene'-Based Fillers: A Review, *Polym. Rev.*, 2018, **58**(3), 403–443, DOI: 10.1080/15583724.2017.1403446.

109 M. Shtein, I. Pri-Bar, M. Varenik and O. Regev, Characterization of Graphene-Nanoplatelets Structure via

Thermogravimetry, *Anal. Chem.*, 2015, **87**(8), 4076–4080, DOI: 10.1021/acs.analchem.5b00228.

110 J. Zhao, S. Pei, W. Ren, L. Gao and H. M. Cheng, Efficient preparation of large-area graphene oxide sheets for transparent conductive films, *ACS Nano*, 2010, **4**(9), 5245–5252, DOI: 10.1021/nn1015506.

111 C. Gómez-Navarro, *et al*. Atomic structure of reduced graphene oxide, *Nano Lett.*, 2010, **10**(4), 1144–1148, DOI: 10.1021/nl9031617.

112 A. T. Najafabadi and E. Gyenge, Synergistic production of graphene microsheets by simultaneous anodic and cathodic electro-exfoliation of graphitic electrodes in aprotic ionic liquids, *Carbon*, 2015, **84**, 449–459, DOI: 10.1016/j.carbon.2014.12.041.

113 K. R. Paton, *et al*. Scalable production of large quantities of defect-free few-layer graphene by shear exfoliation in liquids, *Nat. Mater.*, 2014, **13**, 624–630, DOI: 10.1038/nmat3944.

114 M. Yi and Z. Shen, Kitchen blender for producing high-quality few-layer graphene, *Carbon*, 2014, **78**, 622–626, DOI: 10.1016/j.carbon.2014.07.035.

115 M. V. Bracamonte, G. I. Lacconi, S. E. Urreta and L. E. F. Foa Torres, On the nature of defects in liquid-phase exfoliated graphene, *J. Phys. Chem. C*, 2014, **118**(28), 15455–15459, DOI: 10.1021/jp501930a.

116 M. Yi, Z. Shen, S. Liang, L. Lei, X. Zhang and S. Ma, Water can stably disperse liquid-exfoliated graphene, *Chem. Commun.*, 2013, **49**(94), 11059–11061, DOI: 10.1039/c3cc46457a.

117 T. Shang, G. Feng, Q. Li and Y. Zheng, Production of graphene nanosheets by supercritical CO_2 process coupled with micro-jet exfoliation, *Fullerenes, Nanotubes, Carbon Nanostruct.*, 2017, **25**(12), 691–698, DOI: 10.1080/1536383X.2017.1307832.

118 T. Lin, *et al*. Scotch-tape-like exfoliation of graphite assisted with elemental sulfur and graphene-sulfur composites for high-performance lithium-sulfur batteries, *Energy Environ. Sci.*, 2013, **6**(4), 1283–1290, DOI: 10.1039/c3ee24324a.

119 A. Dato, *et al*. Clean and highly ordered graphene synthesized in the gas phase, *Chem. Commun.*, 2009, **40**, 6095–6097, DOI: 10.1039/b911395a.

120 S. Eigler, *et al*. Wet Chemical Synthesis of Graphene, *Adv. Mater.*, 2013, **25**, 3583–3587, DOI: 10.1002/adma.201300155.

121 B. C. Brodie, On the atomic weight of graphite, *Philos. Trans. R. Soc. London*, 1859, **149**, 249–259.

122 L. Staudenmaier, Verfahren zur Darstellung der Graphitsäure, *Ber. Dtsch. Chem. Ges.*, 1898, **31**(2), 1481–1487.

123 W. S. Hummers and R. E. Offeman, Preparation of Graphitic Oxide, *J. Am. Chem. Soc.*, 1958, **80**(6), 1339.

124 J. Chen, *et al*. Water-enhanced oxidation of graphite to graphene oxide with controlled species of oxygenated groups, *Chem. Sci.*, 2016, **7**(3), 1874–1881, DOI: 10.1039/c5sc03828f.

125 H. Yu, B. Zha, B. Chaoke, R. Li and R. Xing, High-efficient Synthesis of Graphene Oxide Based on Improved Hummers Method, *Sci. Rep.*, 2016, **6**(36143), 1–7, DOI: 10.1038/srep36143.

126 C. Zhu, *et al*. Microbial oxidation of graphite by Acidithiobacillus ferrooxidans CFMI-1, *RSC Adv.*, 2014, **4**(98), 55044–55047, DOI: 10.1039/c4ra09827g.

127 C. Zhu, Q. Hao, Y. Huang, J. Yang and D. Sun, Microbial oxidation of dispersed graphite by nitrifying bacteria 2011.2, *Nanoscale*, 2013, **5**(19), 8982–8985, DOI: 10.1039/c3nr02069j.

128 S. Pei, Q. Wei, K. Huang, H. Cheng and W. Ren, Green synthesis of graphene oxide by seconds timescale water electrolytic oxidation, *Nat. Commun.*, 2018, **9**(145), 1–9, DOI: 10.1038/s41467-017-02479-z.

129 A. Ambrosi and M. Pumera, Electrochemically Exfoliated Graphene and Graphene Oxide for Energy Storage and Electrochemistry Applications, *Chem. – Eur. J.*, 2016, **22**(1), 153–159, DOI: 10.1002/chem.201503110.

130 S. Goswami, P. Banerjee, S. Datta, A. Mukhopadhayay and P. Das, Graphene oxide nanoplatelets synthesized with carbonized agro-waste biomass as green precursor and its application for the treatment of dye rich wastewater, *Process Saf. Environ. Prot.*, 2017, **106**, 163–172, DOI: 10.1016/j.psep.2017.01.003.

131 L. Tang, *et al*. Bottom-up synthesis of large-scale graphene oxide nanosheets, *J. Mater. Chem.*, 2012, **22**(12), 5676–5683, DOI: 10.1039/c2jm15944a.

132 P. P. Brisebois and M. Siaj, Harvesting graphene oxide-years 1859 to 2019: A review of its structure, synthesis, properties and exfoliation, *J. Mater. Chem. C*, 2020, **8**(5), 1517–1547, DOI: 10.1039/c9tc03251g.

133 S. Mao, H. Pu and J. Chen, Graphene oxide and its reduction : modeling and experimental progress, *RSC Adv.*, 2012, **2**, 2643–2662, DOI: 10.1039/c2ra00663d.

134 M. Yan, Pristine graphene: Functionalization, fabrication, and nanocomposite materials, *J. Phys.: Conf. Ser.*, 2018, **1143**, 012012, DOI: 10.1088/1742-6596/1143/1/012012.

135 A. Zurutuza and C. Marinelli, Challenges and opportunities in graphene commercialization, *Nat. Nanotechnol.*, 2014, **9**, 730–734, DOI: 10.1038/nnano.2014.225.

136 S. Eigler, C. Dotzer and A. Hirsch, Visualization of defect densities in reduced graphene oxide, *Carbon*, 2012, **50**(10), 3666–3673, DOI: 10.1016/j.carbon.2012.03.039.

137 B. D. L. Campeon, M. Akada, M. S. Ahmad, Y. Nishikawa, K. Gotoh and Y. Nishina, Non-destructive, uniform, and scalable electrochemical functionalization and exfoliation of graphite, *Carbon*, 2020, **158**, 356–363, DOI: 10.1016/j.carbon.2019.10.085.

138 K. Parvez, *et al*. Exfoliation of Graphite into Graphene in Aqueous Solutions of Inorganic Salts, *J. Am. Chem. Soc.*, 2014, **136**, 6083–6091, DOI: 10.1021/ja5017156.

139 Y. L. Zhong and T. M. Swager, Enhanced Electrochemical Expansion of Graphite for in Situ Electrochemical Functionalization, *J. Am. Chem. Soc.*, 2012, **134**, 17896–17899, DOI: 10.1021/ja309023f.

140 J. Cao, *et al*. Two-Step Electrochemical Intercalation and Oxidation of Graphite for the Mass Production of Graphene Oxide, *J. Am. Chem. Soc.*, 2017, **139**(48), 17446–17456, DOI: 10.1021/jacs.7b08515.

141 A. Ejigu, I. A. Kinloch and R. A. W. Dryfe, Single Stage Simultaneous Electrochemical Exfoliation and Functionalization of Graphene, *ACS Appl. Mater. Interfaces*, 2017, **9**, 710–721, DOI: 10.1021/acsami.6b12868.

142 A. T. Najafabadi and E. Gyenge, High-yield graphene production by electrochemical exfoliation of graphite: Novel ionic liquid (IL)–acetonitrile electrolyte with low IL content, *Carbon*, 2014, **71**, 58–69, DOI: 10.1016/j.carbon.2014.01.012.

143 C. T. J. Low, F. C. Walsh, M. H. Chakrabarti, M. A. Hashim and M. A. Hussain, Electrochemical approaches to the production of graphene flakes and their potential applications, *Carbon*, 2013, **54**, 1–21, DOI: 10.1016/j.carbon.2012.11.030.

144 Y. Lv, L. Yu, C. Jiang, S. Chen and Z. Nie, Synthesis of graphene nanosheet powder with layer number control via a soluble salt-assisted route, *RSC Adv.*, 2014, **4**(26), 13350–13354, DOI: 10.1039/c3ra45060k.

145 S. Liang, M. Yi, Z. Shen, L. Liu, X. Zhang and S. Ma, One-step green synthesis of graphene nanomesh by fluid-based method, *RSC Adv.*, 2014, **4**(31), 16127–16131, DOI: 10.1039/c4ra01250j.

146 A. Dato, V. Radmilovic, Z. Lee, J. Phillips and M. Frenklach, Substrate-free gas-phase synthesis of graphene sheets, *Nano Lett.*, 2008, **8**(7), 2012–2016, DOI: 10.1021/nl8011566.

147 O. Y. Posudievsky, O. A. Khazieieva, V. G. Koshechko, V. D. Pokhodenko and V. V. Cherepanov, High yield of graphene by dispersant-free liquid exfoliation of mechanochemically delaminated graphite, *J. Nanopart. Res.*, 2013, **15**, 2046, DOI: 10.1007/s11051-013-2046-y.

148 V. M. Samoilov, *et al*. Formation of graphene aqueous suspensions using fluorinated surfactant-assisted ultrasonication of pristine graphite, *Carbon*, 2015, **84**, 38–46, DOI: 10.1016/j.carbon.2014.11.051.

149 L. Guardia, *et al*. High-throughput production of pristine graphene in an aqueous dispersion assisted by non-ionic surfactants, *Carbon*, 2011, **49**(5), 1653–1662, DOI: 10.1016/j.carbon.2010.12.049.

150 Z. Sun, J. Masa, Z. Liu, W. Schuhmann and M. Muhler, Highly concentrated aqueous dispersions of graphene exfoliated by sodium taurodeoxycholate: Dispersion behavior and potential application as a catalyst support for the oxygen-reduction reaction, *Chem. – Eur. J.*, 2012, **18**(22), 6972–6978, DOI: 10.1002/chem.201103253.

151 R. J. Smith, M. Lotya and J. N. Coleman, The importance of repulsive potential barriers for the dispersion of graphene using surfactants, *New J. Phys.*, 2010, **12**, 125008, DOI: 10.1088/1367-2630/12/12/125008.

152 J. W. T. Seo, A. A. Green, A. L. Antaris and M. C. Hersam, High-concentration aqueous dispersions of graphene using nonionic, biocompatible block copolymers, *J. Phys. Chem. Lett.*, 2011, **2**(9), 1004–1008, DOI: 10.1021/jz2003556.

153 M. Lotya, P. J. King, U. Khan, S. De and J. N. Coleman, High-concentration, surfactant-stabilized graphene dispersions, *ACS Nano*, 2010, **4**(6), 3155–3162, DOI: 10.1021/nn1005304.

154 T. Skaltsas, X. Ke, C. Bittencourt and N. Tagmatarchis, Ultrasonication induces oxygenated species and defects onto exfoliated graphene, *J. Phys. Chem. C*, 2013, **117**(44), 23272–23278, DOI: 10.1021/jp4057048.

155 E. Y. Polyakova, *et al*. Scanning tunneling microscopy and X-ray photoelectron spectroscopy studies of graphene films prepared by sonication-assisted dispersion, *ACS Nano*, 2011, **5**(8), 6102–6108, DOI: 10.1021/nn1009352.

156 M. Lotya, *et al*. Liquid phase production of graphene by exfoliation of graphite in surfactant/water solutions, *J. Am. Chem. Soc.*, 2009, **131**(10), 3611–3620, DOI: 10.1021/ja807449u.

157 R. Kabe, X. Feng, C. Adachi and K. Müllen, Exfoliation of graphite into graphene in polar solvents mediated by amphiphilic hexa-peri-hexabenzocoronene, *Chem. – Asian J.*, 2014, **9**(11), 3125–3129, DOI: 10.1002/asia.201402535.

158 A. A. Green and M. C. Hersam, Solution phase production of graphene with controlled thickness via density differentiation, *Nano Lett.*, 2009, **9**(12), 4031–4036, DOI: 10.1021/nl902200b.

159 W. Zhao, M. Fang, F. Wu, H. Wu, L. Wang and G. Chen, Preparation of graphene by exfoliation of graphite using wet ball milling, *J. Mater. Chem.*, 2010, **20**(28), 5817–5819, DOI: 10.1039/c0jm01354d.

160 C. Knieke, A. Berger, M. Voigt, R. N. Klupp Taylor, J. Röhrl and W. Peukert, Scalable production of graphene sheets by mechanical delamination, *Carbon*, 2010, **48**(11), 3196–3204, DOI: 10.1016/j.carbon.2010.05.003.

161 B. Yang, *et al.*, *US Pat.*, 0010325, 2020.

162 M. Yi, J. Li, Z. Shen, X. Zhang and S. Ma, Morphology and structure of mono- and few-layer graphene produced by jet cavitation, *Appl. Phys. Lett.*, 2011, **99**(12), 123112, DOI: 10.1063/1.3641863.

163 M. Buzaglo, M. Shtein and O. Regev, Graphene Quantum Dots Produced by Microfluidization, *Chem. Mater.*, 2016, **28**(1), 21–24, DOI: 10.1021/acs.chemmater.5b03301.

164 Y. Wei and Z. Sun, Liquid-phase exfoliation of graphite for mass production of pristine few-layer graphene, *Curr. Opin. Colloid Interface Sci.*, 2015, **20**(5–6), 311–321, DOI: 10.1016/j.cocis.2015.10.010.

165 C. Gómez-Navarro, M. Burghard and K. Kern, Elastic Properties of Chemically Derived Single Graphene Sheets, *Nano Lett.*, 2008, **8**(7), 2045–2049, DOI: 10.1021/nl801384y.

166 Y. Liu, *et al*., Graphene enhanced flexible expanded graphite film with high electric, thermal conductivities and EMI shielding at low content, *Carbon*, 2018, **133**, 435–445, DOI: 10.1016/j.carbon.2018.03.047.

167 K. Muthoosamy and S. Manickam, State of the art and recent advances in the ultrasound-assisted synthesis, exfo-

liation and functionalization of graphene derivatives, *Ultrason. Sonochem.*, 2017, **39**, 478–493, DOI: 10.1016/j.ultsonch.2017.05.019.

168 M. Yi and Z. Shen, A review on mechanical exfoliation for the scalable production of graphene, *J. Mater. Chem. A*, 2015, **3**(22), 11700–11715, DOI: 10.1039/c5ta00252d.

169 T. Lin, *et al.*, Facile and economical exfoliation of graphite for mass production of high-quality graphene sheets, *J. Mater. Chem. A*, 2013, **1**(3), 500–504, DOI: 10.1039/c2ta00518b.

170 X. Li, J. Shen, C. Wu and K. Wu, Ball-Mill-Exfoliated Graphene: Tunable Electrochemistry and Phenol Sensing, *Small*, 2019, **15**(48), 1805567, DOI: 10.1002/smll.201805567.

171 M. Buzaglo, I. P. Bar, M. Varenik, L. Shunak, S. Pevzner and O. Regev, Graphite-to-Graphene: Total Conversion, *Adv. Mater.*, 2017, **29**(8), 1603528, DOI: 10.1002/adma.201603528.

172 S. Deng, X. Dong Qi, Y. Ling Zhu, H. Ju Zhou, F. Chen and Q. Fu, A facile way to large-scale production of few-layered graphene via planetary ball mill, *Chin. J. Polym. Sci.*, 2016, **34**, 1270–1280, DOI: 10.1007/s10118-016-1836-y.

173 C. Backes, *et al.*, Production and processing of graphene and related materials, *2D Mater.*, 2020, **7**(2), 022001, DOI: 10.1088/2053-1583/AB1E0A.

174 W. Yan, M. Vijay, A. Tieu, M. Xu and B. Daniels, *US Pat.*, 10640383, 2020.

175 Q. Q. Xu, *et al.*, The production of graphene using impinging jet exfoliation in a binary system of CO_2 and N-methyl pyrrolidone, *Nanotechnology*, 2020, **31**(26), 265601, DOI: 10.1088/1361-6528/ab7f7c.

176 A. Dato, Graphene synthesized in atmospheric plasmas - A review, *J. Mater. Res.*, 2019, **34**(1), 214–230, DOI: 10.1557/jmr.2018.470.

177 S. A. Eremin, *et al.*, Growth of Allotropic Modifications of Carbon on a Thin Tungsten Wire from Vapor Phase with the Use of Microwave Plasma, *Inorg. Mater. Appl. Res.*, 2020, **11**, 568–571, DOI: 10.1134/S2075113320030120.

178 H. Döscher, T. Schmaltz, C. Neef, A. Thielmann and T. Reiss, Graphene Roadmap Briefs (No. 2): industrialization status and prospects 2020, *2D Mater.*, 2021, **8**(2), 022005, DOI: 10.1088/2053-1583/abddcd.

179 T. Reiss, K. Hjelt and A. C. Ferrari, Graphene is on track to deliver on its promises, *Nat. Nanotechnol.*, 2019, **14**, 907–910, DOI: 10.1038/s41565-019-0557-0.

180 L. Serrano-Luján, *et al.*, Environmental impact of the production of graphene oxide and reduced graphene oxide, *SN Appl. Sci.*, 2019, **1**, 179, DOI: 10.1007/s42452-019-0193-1.

181 L. Fusco, *et al.*, Skin irritation potential of graphene-based materials using a non-animal test, *Nanoscale*, 2020, **12**(2), 610–622, DOI: 10.1039/c9nr06815e.

182 R. Bhargava, S. Khan, M. M. N. Ansari and N. Ahmad, Green synthesis approach for the reduction of graphene oxide by using glucose, *AIP Conf. Proc.*, 2019, **2115**(1), 030075, DOI: 10.1063/1.5112914.

183 A. M. Díez-Pascual and A. L. Díez-Vicente, Poly(propylene fumarate)/Polyethylene Glycol-Modified Graphene Oxide Nanocomposites for Tissue Engineering, *ACS Appl. Mater. Interfaces*, 2016, **8**(28), 17902–17914, DOI: 10.1021/acsami.6b05635.

184 J. Zhao, *et al.*, Graphene oxide-based antibacterial cotton fabrics, *Adv. Healthcare Mater.*, 2013, **2**(9), 1259–1266, DOI: 10.1002/adhm.201200437.

185 X. Zhi, *et al.*, The immunotoxicity of graphene oxides and the effect of PVP-coating, *Biomaterials*, 2013, **34**(21), 5254–5261, DOI: 10.1016/j.biomaterials.2013.03.024.

186 J. Frontiñán-Rubio, M. Victoria Gómez, C. Martín, J. M. González-Domínguez, M. Durán-Prado and E. Vázquez, Differential effects of graphene materials on the metabolism and function of human skin cells, *Nanoscale*, 2018, **10**(24), 11604–11615, DOI: 10.1039/c8nr00897c.

187 T. Pulingam, *et al.*, Synergistic antibacterial actions of graphene oxide and antibiotics towards bacteria and the toxicological effects of graphene oxide on human epidermal keratinocytes, *Eur. J. Pharm. Sci.*, 2020, **142**, 105087, DOI: 10.1016/j.ejps.2019.105087.

188 T. Sukumar, *et al.*, Cytotoxicity of Formulated Graphene and Its Natural Rubber Nanocomposite Thin Film in Human Vaginal Epithelial Cells: An Influence of Noncovalent Interaction, *ACS Biomater. Sci. Eng.*, 2020, **6**(4), 2007–2019, DOI: 10.1021/acsbiomaterials.9b01897.

189 A. B. Seabra, A. J. Paula, R. De Lima, O. L. Alves and N. Durán, Nanotoxicity of graphene and graphene oxide, *Chem. Res. Toxicol.*, 2014, **27**(2), 159–168, DOI: 10.1021/tx400385x.

190 A. Bianco and M. Prato, Safety concerns on graphene and 2D materials: A Flagship perspective, *2D Mater.*, 2015, **2**(3), 030201, DOI: 10.1088/2053-1583/2/3/030201.

191 R. Arvidsson, S. Molander and B. A. Sandén, Review of Potential Environmental and Health Risks of the Nanomaterial Graphene, *Hum. Ecol. Risk Assess.*, 2013, **19**(4), 873–887, DOI: 10.1080/10807039.2012.702039.

192 Y. Volkov, J. McIntyre and A. Prina-Mello, Graphene toxicity as a double-edged sword of risks and exploitable opportunities: A critical analysis of the most recent trends and developments, *2D Mater.*, 2017, **4**(2), 022001, DOI: 10.1088/2053-1583/aa5476.

193 E. T. Nadres, J. Fan and D. F. Rodrigues, Toxicity and Environmental Applications of Graphene-Based Nanomaterials, in *Graphene based materials in health and environment*, ed. G. Gonçalves, P. Marques and M. Vila, Springer, Cham, 2016, pp. 323–356.

194 G. Lalwani, W. Xing and B. Sitharaman, Enzymatic degradation of oxidized and reduced graphene nanoribbons by lignin peroxidase, *J. Mater. Chem. B*, 2014, **2**(37), 6354–6362, DOI: 10.1039/c4tb00976b.

195 Y. Lin, J. Zeng, J. Ma and J. Gong, Preparation and Property of Waterborne Polyurethane/Cellulose Nanofiber Nanocomposite Films, *Mater. Sci. Forum*, 2020, **993**, 631–637, DOI: 10.4028/www.scientific.net/MSF.993.631.

196 L. Zhang, H. Zhang and J. Guo, Synthesis and properties of UV-curable polyester-based waterborne polyurethane/functionalized silica composites and morphology of their nanostructured films, *Ind. Eng. Chem. Res.*, 2012, **51**(25), 8434–8441, DOI: 10.1021/ie3000248.

197 S. Awad, *et al.*, Free volumes, glass transitions, and cross-links in zinc oxide/waterborne polyurethane nanocomposites, *Macromolecules*, 2011, **44**(1), 29–38, DOI: 10.1021/ma102366d.

198 Z.-F. Li, S.-J. Wang and J.-Y. Li, Synthesis and characterization of waterborne polyurethane/organic clay nanocomposites, *Front. Mater. Sci.*, 2008, **2**(3), 271–275, DOI: 10.1007/s11706-008-0056-y.

199 S. Prasertsri and N. Rattanasom, Mechanical and damping properties of silica/natural rubber composites prepared from latex system, *Polym. Test.*, 2011, **30**(5), 515–526, DOI: 10.1016/j.polymertesting.2011.04.001.

200 S. Prasertsri and N. Rattanasom, Fumed and precipitated silica reinforced natural rubber composites prepared from latex system: Mechanical and dynamic properties, *Polym. Test.*, 2012, **31**(5), 593–605, DOI: 10.1016/j.polymertesting.2012.03.003.

201 A. Tohsan, P. Phinyocheep, S. Kittipoom, W. Pattanasiriwisawa and Y. Ikeda, Novel biphasic structured composite prepared by in situ silica filling in natural rubber latex, *Polym. Adv. Technol.*, 2012, **23**(10), 1335–1342, DOI: 10.1002/pat.2051.

202 A. Kongsinlark, G. L. Rempel and P. Prasassarakich, Synthesis of monodispersed polyisoprene-silica nanoparticles via differential microemulsion polymerization and mechanical properties of polyisoprene nanocomposite, *Chem. Eng. J.*, 2012, **193–194**, 215–226, DOI: 10.1016/j.cej.2012.04.008.

203 Z. F. Wang, *et al.*, The impact of esterification on the properties of starch/natural rubber composite, *Compos. Sci. Technol.*, 2009, **69**(11–12), 1797–1803, DOI: 10.1016/j.compscitech.2009.04.018.

204 C. M. Deng, M. Chen, N. J. Ao, D. Yan and Z. Q. Zheng, $CaCO_3$/natural rubber latex nanometer composite and its properties, *J. Appl. Polym. Sci.*, 2006, **101**(5), 3442–3447, DOI: 10.1002/app.24345.

205 Y. T. Vu, J. E. Mark, L. H. Pham and M. Engelhardt, Clay nanolayer reinforcement of cis-1,4-polyisoprene and epoxidized natural rubber, *J. Appl. Polym. Sci.*, 2001, **82**(6), 1391–1403, DOI: 10.1002/app.1976.

206 E. Abraham, *et al.*, Physicomechanical properties of nanocomposites based on cellulose nanofibre and natural rubber latex, *Cellulose*, 2013, **20**, 417–427, DOI: 10.1007/s10570-012-9830-1.

207 N. Rattanasom, U. Thammasiripong and K. Suchiva, Mechanical properties of deproteinized natural rubber in comparison with synthetic cis-1, 4 polyisoprene vulcanizates: Gum and black-filled vulcanizates, *J. Appl. Polym. Sci.*, 2005, **97**(3), 1139–1144, DOI: 10.1002/app.21781.

208 N. S. M. El-Tayeb and R. M. Nasir, Effect of soft carbon black on tribology of deproteinised and polyisoprene rubbers, *Wear*, 2007, **262**(3–4), 350–361, DOI: 10.1016/j.wear.2006.05.021.

209 Z. Peng, C. Feng, Y. Luo, Y. Li and L. X. Kong, Self-assembled natural rubber/multi-walled carbon nanotube composites using latex compounding techniques, *Carbon*, 2010, **48**(15), 4497–4503, DOI: 10.1016/j.carbon.2010.08.025.

210 K. A. Anand, T. S. Jose, R. Alex and R. Joseph, Natural rubber-carbon nanotube composites through latex compounding, *Int. J. Polym. Mater.*, 2010, **59**(1), 33–44, DOI: 10.1080/00914030903172916.

211 Y. H. Zhan, G. Q. Liu, H. S. Xia and N. Yan, Natural rubber/carbon black/carbon nanotubes composites prepared through ultrasonic assisted latex mixing process, *Plast., Rubber Compos.*, 2011, **40**(1), 32–39, DOI: 10.1179/174328911X12940139029284.

212 N. Yan, J. K. Wu, Y. H. Zhan and H. S. Xia, Carbon nanotubes/carbon black synergistic reinforced natural rubber composites, *Plast., Rubber Compos.*, 2009, **38**(7), 290–296, DOI: 10.1179/146580109X12473409436580.

213 J. Kwon and H. Kim, Comparison of the properties of waterborne polyurethane/multiwalled carbon nanotube and acid-treated multiwalled carbon nanotube composites prepared by in situ polymerization, *J. Polym. Sci., Part A: Polym. Chem.*, 2005, **43**(17), 3973–3985, DOI: 10.1002/pola.20897.

214 H. C. Kuan, C. C. M. Ma, W. P. Chang, S. M. Yuen, H. H. Wu and T. M. Lee, Synthesis, thermal, mechanical and rheological properties of multiwall carbon nanotube/waterborne polyurethane nanocomposite, *Compos. Sci. Technol.*, 2005, **65**(11–12), 1703–1710, DOI: 10.1016/j.compscitech.2005.02.017.

215 Y. Nakaramontri, S. Pichaiyut, S. Wisunthorn and C. Nakason, Hybrid carbon nanotubes and conductive carbon black in natural rubber composites to enhance electrical conductivity by reducing gaps separating carbon nanotube encapsulates, *Eur. Polym. J.*, 2017, **90**, 467–484, DOI: 10.1016/j.eurpolymj.2017.03.029.

216 A. Arzac, G. P. Leal, J. C. de la Cal and R. Tomovska, Water-Borne Polymer/Graphene Nanocomposites, *Macromol. Mater. Eng.*, 2017, **302**(1), 1600315, DOI: 10.1002/mame.201600315.

217 E. Bourgeat-Lami, J. Faucheu and A. Noël, Latex routes to graphene-based nanocomposites, *Polym. Chem.*, 2015, **6**(30), 5323–5357, DOI: 10.1039/c5py00490j.

218 M. Iliut, C. Silva, S. Herrick, M. McGlothlin and A. Vijayaraghavan, Graphene and water-based elastomers thin-film composites by dip-moulding, *Carbon*, 2016, **106**, 228–232, DOI: 10.1016/j.carbon.2016.05.032.

219 N. Yousefi, M. M. Gudarzi, Q. Zheng, S. H. Aboutalebi, F. Sharif and J. K. Kim, Self-alignment and high electrical conductivity of ultralarge graphene oxide-polyurethane nanocomposites, *J. Mater. Chem.*, 2012, **22**(25), 12709–12717, DOI: 10.1039/c2jm30590a.

220 J. Hu and F. Zhang, Self-assembled fabrication and flame-retardant properties of reduced graphene oxide/water-

borne polyurethane nanocomposites, *J. Therm. Anal. Calorim.*, 2014, **118**, 1561–1568, DOI: 10.1007/s10973-014-4078-7.

221 F. P. Leng, L. P. Lim, L. K. Goh, Y. Y. Loh, J. C. Juan and N. M. Huang, *US Pat.*, 0270863, 2019.

222 C. Bernard, *et al.*, Graphene oxide/waterborne polyurethane nanocoatings: effects of graphene oxide content on performance properties, *J. Coat. Technol. Res.*, 2020, **17**(1), 255–269, DOI: 10.1007/s11998-019-00267-6.

223 D. Spasevska, V. Daniloska, G. P. Leal, J. B. Gilev and R. Tomovska, Reactive emulsion mixing as a novel pathway toward water-borne reduced graphene oxide/polymer composites, *RSC Adv.*, 2014, **4**(47), 24477–24483, DOI: 10.1039/c4ra01487a.

224 J. R. Potts, O. Shankar, L. Du and R. S. Ruoff, Processing-morphology-property relationships and composite theory analysis of reduced graphene oxide/natural rubber nanocomposites, *Macromolecules*, 2012, **45**(15), 6045–6055, DOI: 10.1021/ma300706k.

225 Z. Tang, X. Wu, B. Guo, L. Zhang and D. Jia, Preparation of butadiene-styrene-vinyl pyridine rubber-graphene oxide hybrids through co-coagulation process and in situ interface tailoring, *J. Mater. Chem.*, 2012, **22**(15), 7492–7501, DOI: 10.1039/c2jm00084a.

226 G. Scherillo, *et al.*, Tailoring assembly of reduced graphene oxide nanosheets to control gas barrier properties of natural rubber nanocomposites, *ACS Appl. Mater. Interfaces*, 2014, **6**(4), 2230–2234, DOI: 10.1021/am405768m.

227 A. Mohamed, *et al.*, Graphene-philic surfactants for nanocomposites in latex technology, *Adv. Colloid Interface Sci.*, 2016, **230**, 54–69, DOI: 10.1016/j.cis.2016.01.003.

228 A. Arzac, G. P. Leal, R. Fajgar and R. Tomovska, Comparison of the emulsion mixing and in situ polymerization techniques for synthesis of water-borne reduced graphene oxide/polymer composites: Advantages and drawbacks, *Part. Part. Syst. Charact.*, 2014, **31**(1), 143–151, DOI: 10.1002/ppsc.201300286.

229 Y. R. Lee, A. V. Raghu, H. M. Jeong and B. K. Kim, Properties of waterborne polyurethane/functionalized graphene sheet nanocomposites prepared by an in situ method, *Macromol. Chem. Phys.*, 2009, **210**(15), 1247–1254, DOI: 10.1002/macp.200900157.

230 S. C. Thickett, N. Wood, Y. H. Ng and P. B. Zetterlund, Hollow hybrid polymer-graphene oxide nanoparticles via Pickering miniemulsion polymerization, *Nanoscale*, 2014, **6**(15), 8590–8594, DOI: 10.1039/c4nr01175a.

231 J. Feng, X. Wang, P. Guo, Y. Wang and X. Luo, Mechanical properties and wear resistance of sulfonated graphene/waterborne polyurethane composites prepared by in situ method, *Polymers*, 2018, **10**(1), 75, DOI: 10.3390/polym10010075.

232 A. S. Patole, S. P. Patole, H. Kang, J. B. Yoo, T. H. Kim and J. H. Ahn, A facile approach to the fabrication of graphene/polystyrene nanocomposite by in situ micro-emulsion polymerization, *J. Colloid Interface Sci.*, 2010, **350**(2), 530–537, DOI: 10.1016/j.jcis.2010.01.035.

233 Z. Yang, H. Liu, S. Wu, Z. Tang, B. Guo and L. Zhang, A green method for preparing conductive elastomer composites with interconnected graphene network via Pickering emulsion templating, *Chem. Eng. J.*, 2018, **342**, 112–119, DOI: 10.1016/j.cej.2018.02.079.

234 A. Pazat, E. Beyou, C. Barrès, F. Bruno and C. Janin, In situ emulsion cationic polymerization of isoprene onto the surface of graphite oxide sheets, *Appl. Surf. Sci.*, 2017, **396**, 902–911, DOI: 10.1016/j.apsusc.2016.11.059.

235 H. Xu, *et al.*, Influence of processing conditions on dispersion, electrical and mechanical properties of graphene-filled-silicone rubber composites, *Composites, Part A*, 2016, **91**, 53–64, DOI: 10.1016/j.compositesa.2016.09.011.

236 D. Chen and G. Chen, In situ synthesis of thermoplastic polyurethane/graphene nanoplatelets conductive composite by ball milling, *J. Reinf. Plast. Compos.*, 2013, **32**(5), 300–307, DOI: 10.1177/0731684412471230.

237 I. A. Kinloch, J. Suhr, J. Lou, R. J. Young and P. M. Ajayan, Composites with carbon nanotubes and graphene: An outlook, *Science*, 2018, **362**(6414), 547–553, DOI: 10.1126/science.aat7439.

238 Y. J. Kim and B. K. Kim, Synthesis and properties of silanized waterborne polyurethane/graphene nanocomposites, *Colloid Polym. Sci.*, 2014, **292**, 51–58, DOI: 10.1007/s00396-013-3054-2.

239 R. Zhou, P. Li, Z. Fan, D. Du and J. Ouyang, Stretchable heaters with composites of an intrinsically conductive polymer, reduced graphene oxide and an elastomer for wearable thermotherapy, *J. Mater. Chem. C*, 2017, **5**(6), 1544–1551, DOI: 10.1039/c6tc04849h.

240 D. La, *et al.*, A New Approach of Fabricating Graphene Nanoplates@Natural Rubber Latex Composite and Its Characteristics and Mechanical Properties, *J. Carbon Res.*, 2018, **4**(3), 50, DOI: 10.3390/c4030050.

241 M. B. Kale, *et al.*, Waterborne polyurethane/graphene oxide-silica nanocomposites with improved mechanical and thermal properties for leather coatings using screen printing, *Polymer*, 2019, **170**, 43–53, DOI: 10.1016/j.polymer.2019.02.055.

242 N. Yan, H. Xia, Y. Zhan and G. Fei, New insights into fatigue crack growth in graphene-filled natural rubber composites by microfocus hard-X-ray beamline radiation, *Macromol. Mater. Eng.*, 2013, **298**(1), 38–44, DOI: 10.1002/mame.201200044.

243 K. Y. Chong, C. H. Chia, S. Zakaria, T. H. Pham, D. Lucas and S. X. Chin, Puncture resistance and mechanical properties of graphene oxide reinforced natural rubber latex, *Sains Malays.*, 2018, **47**(9), 2171–2178, DOI: 10.17576/jsm-2018-4709-27.

244 S. H. Yoon, J. H. Park, E. Y. Kim and B. K. Kim, Preparations and properties of waterborne polyurethane/allyl isocyanated-modified graphene oxide nano-

composites, *Colloid Polym. Sci.*, 2011, **289**, 1809–1814, DOI: 10.1007/s00396-011-2498-5.

245 S. H. Choi, *et al.*, Properties of Graphene/Waterborne Polyurethane Nanocomposites Cast from Colloidal Dispersion Mixtures, *J. Macromol. Sci., Part B: Phys.*, 2012, **51**(1), 197–207, DOI: 10.1080/00222348.2011.583193.

246 L. P. Lim, J. C. Juan, N. M. Huang, L. K. Goh, F. P. Leng and Y. Y. Loh, Enhanced tensile strength and thermal conductivity of natural rubber graphene composite properties via rubber-graphene interaction, *Mater. Sci. Eng., B*, 2019, **246**, 112–119, DOI: 10.1016/j.mseb.2019.06.004.

247 G. George, *et al.*, Thermally conductive thin films derived from defect free graphene-natural rubber latex nanocomposite: Preparation and properties, *Carbon*, 2017, **119**, 527–534, DOI: 10.1016/j.carbon.2017.04.068.

248 T. Wan and D. Chen, Mechanical enhancement of self-healing waterborne polyurethane by graphene oxide, *Prog. Org. Coat.*, 2018, **121**, 73–79, DOI: 10.1016/j.porgcoat.2018.04.016.

249 A. V. Raghu, Y. R. Lee, H. M. Jeong and C. M. Shin, Preparation and physical properties of waterborne polyurethane/functionalized graphene sheet nanocomposites, *Macromol. Chem. Phys.*, 2008, **209**(24), 2487–2493, DOI: 10.1002/macp.200800395.

250 J. Yang, *et al.*, Synthesis and properties of polydimethylsiloxane/graphene oxide modified, water-based polyurethane/polyacrylate, *J. Appl. Polym. Sci.*, 2019, **136**(36), 47926, DOI: 10.1002/app.47926.

251 P. Zhang, P. Xu, H. Fan, Z. Sun and J. Wen, Covalently functionalized graphene towards molecular-level dispersed waterborne polyurethane nanocomposite with balanced comprehensive performance, *Appl. Surf. Sci.*, 2019, **471**, 595–606, DOI: 10.1016/j.apsusc.2018.11.235.

252 Y. Zhan, J. Wu, H. Xia, N. Yan, G. Fei and G. Yuan, Dispersion and exfoliation of graphene in rubber by an ultrasonically-assisted latex mixing and in situ reduction process, *Macromol. Mater. Eng.*, 2011, **296**(7), 590–602, DOI: 10.1002/mame.201000358.

253 L. Wu, P. Qu, R. Zhou, B. Wang and S. Liao, Green synthesis of reduced graphene oxide and its reinforcing effect on natural rubber composites, *High Perform. Polym.*, 2015, **27**(4), 486–496, DOI: 10.1177/0954008314555530.

254 H. Aguilar-Bolados, J. Brasero, M. A. Lopez-Manchado and M. Yazdani-Pedram, High performance natural rubber/thermally reduced graphite oxide nanocomposites by latex technology, *Composites, Part B*, 2014, **67**, 449–454, DOI: 10.1016/j.compositesb.2014.08.010.

255 L. Zhao, X. Sun, Q. Liu, J. Zhao and W. Xing, Natural Rubber/Graphene Oxide Nanocomposites Prepared by Latex Mixing, *J. Macromol. Sci., Part B: Phys.*, 2015, **54**(5), 581–592, DOI: 10.1080/00222348.2015.1019325.

256 C. Zhang, T. Zhai, Y. Dan and L. S. Turng, Reinforced natural rubber nanocomposites using graphene oxide as a reinforcing agent and their in situ reduction into highly conductive materials, *Polym. Compos.*, 2017, **38**, E199–E207, DOI: 10.1002/pc.23972.

257 A. Mohamed, *et al.*, Rational design of aromatic surfactants for graphene/natural rubber latex nanocomposites with enhanced electrical conductivity, *J. Colloid Interface Sci.*, 2018, **516**, 34–47, DOI: 10.1016/j.jcis.2018.01.041.

258 H. Aguilar-Bolados, M. A. Lopez-Manchado, J. Brasero, F. Avilés and M. Yazdani-Pedram, Effect of the morphology of thermally reduced graphite oxide on the mechanical and electrical properties of natural rubber nanocomposites, *Composites, Part B*, 2016, **87**, 350–356, DOI: 10.1016/j.compositesb.2015.08.079.

259 B. Dong, L. Zhang and Y. Wu, Highly conductive natural rubber–graphene hybrid films prepared by solution casting and in situ reduction for solvent-sensing application, *J. Mater. Sci.*, 2016, **51**, 10561–10573, DOI: 10.1007/s10853-016-0276-y.

260 K. Tian, Z. Su, H. Wang, X. Tian, W. Huang and C. Xiao, N-doped reduced graphene oxide/waterborne polyurethane composites prepared by in situ chemical reduction of graphene oxide, *Composites, Part A*, 2017, **94**, 41–49, DOI: 10.1016/j.compositesa.2016.11.020.

261 X. Luo, P. Zhang, R. Liu, W. Li, B. Ge and M. Cao, Preparation and physical properties of functionalized graphene/waterborne polyurethane UV-curing composites by click chemistry, *Polym. Int.*, 2016, **65**(4), 415–422, DOI: 10.1002/pi.5070.

262 J. Li, *et al.*, Self-assembled graphene oxide microcapsules in Pickering emulsions for self-healing waterborne polyurethane coatings, *Compos. Sci. Technol.*, 2017, **151**, 282–290, DOI: 10.1016/j.compscitech.2017.07.031.

263 S. T. Hsiao, *et al.*, Using a non-covalent modification to prepare a high electromagnetic interference shielding performance graphene nanosheet/water-borne polyurethane composite, *Carbon*, 2013, **60**, 57–66, DOI: 10.1016/j.carbon.2013.03.056.

264 F. Zhang, *et al.*, Applications of hydrophobic α,ω-bis(amino)-terminated polydimethylsiloxane-graphene oxide in enhancement of anti-corrosion ability of waterborne polyurethane, *Colloids Surf., A*, 2020, **600**, 124981, DOI: 10.1016/j.colsurfa.2020.124981.

265 G. Christopher, M. Anbu Kulandainathan and G. Harichandran, Comparative study of effect of corrosion on mild steel with waterborne polyurethane dispersion containing graphene oxide versus carbon black nanocomposites, *Prog. Org. Coat.*, 2015, **89**, 199–211, DOI: 10.1016/j.porgcoat.2015.09.022.

266 H. Kim and S. Lee, Electrical properties of graphene/waterborne polyurethane composite films, *Fibers Polym.*, 2017, **18**, 1304–1313, DOI: 10.1007/s12221-017-7142-7.

267 H. Kim, S. Lee and H. Kim, Electrical Heating Performance of Electro-Conductive Para-aramid Knit Manufactured by Dip-Coating in a Graphene/Waterborne Polyurethane Composite, *Sci. Rep.*, 2019, **9**, 1511, DOI: 10.1038/s41598-018-37455-0.

268 W. Song, B. Wang, L. Fan, F. Ge and C. Wang, Graphene oxide/waterborne polyurethane composites for fine pattern fabrication and ultrastrong ultraviolet protection

cotton fabric via screen printing, *Appl. Surf. Sci.*, 2019, **463**, 403–411, DOI: 10.1016/j.apsusc.2018.08.167.

269 H. Kim and S. Lee, Evaluation of Laundering Durability of Electro-conductive Textile Dip-coated on Para Aramid Knit with Graphene/Waterborne Polyurethane Composite, *Fibers Polym.*, 2018, **19**, 2351–2358, DOI: 10.1007/s12221-018-8591-3.

270 B. B. Shaun, R. Cai, X. Sun, C. Huang, S. Bi and J. Ran, Strain sensing properties of graphene/elastic fabric, *IOP Conf. Ser.: Mater. Sci. Eng.*, 2020, **774**, 012122, DOI: 10.1088/1757-899X/774/1/012122.

271 H. Zhu, Y. Yang, A. Sheng, H. Duan, G. Zhao and Y. Liu, Layered structural design of flexible waterborne polyurethane conductive film for excellent electromagnetic interference shielding and low microwave reflectivity, *Appl. Surf. Sci.*, 2019, **469**, 1–9, DOI: 10.1016/j.apsusc.2018.11.007.

272 T. Wang, *et al.*, Tannic acid modified graphene/CNT three-dimensional conductive network for preparing high-performance transparent flexible heaters, *J. Colloid Interface Sci.*, 2020, **577**, 300–310, DOI: 10.1016/j.jcis.2020.05.084.

273 S. T. Hsiao, *et al.*, Lightweight and flexible reduced graphene oxide/water-borne polyurethane composites with high electrical conductivity and excellent electromagnetic interference shielding performance, *ACS Appl. Mater. Interfaces*, 2014, **6**(13), 10667–10678, DOI: 10.1021/am502412q.

274 E. J. Shin and S. M. Choi, Advances in Waterborne Polyurethane-Based Biomaterials for Biomedical Applications, in *Novel Biomaterials for regenerative medicine, Advances in Experimental Medicine and Biology*, ed. H. Chun, K. Park, C. H. Kim and G. Khang, Springer, Singapore, 2018, vol. 1077, pp. 251–283.

275 Y. J. Wang, U. S. Jeng and S. H. Hsu, Biodegradable Water-Based Polyurethane Shape Memory Elastomers for Bone Tissue Engineering, *ACS Biomater. Sci. Eng.*, 2018, **4**(4), 1397–1406, DOI: 10.1021/acsbiomaterials.8b00091.

276 T. H. Lee, C. T. Yen and S. H. Hsu, Preparation of Polyurethane-Graphene Nanocomposite and Evaluation of Neurovascular Regeneration, *ACS Biomater. Sci. Eng.*, 2020, **6**(1), 597–609, DOI: 10.1021/acsbiomaterials.9b01473.

277 P. Miao, J. Wang, C. Zhang, M. Sun, S. Cheng and H. Liu, Graphene Nanostructure-Based Tactile Sensors for Electronic Skin Applications, *Nano-Micro Lett.*, 2019, **11**(71), 1–37, DOI: 10.1007/s40820-019-0302-0.

278 B. Dong, S. Wu, L. Zhang and Y. Wu, High performance natural rubber composites with well-organized interconnected graphene networks for strain-sensing application, *Ind. Eng. Chem. Res.*, 2016, **55**(17), 4919–4929, DOI: 10.1021/acs.iecr.6b00214.

279 A. Mirmohseni, M. Azizi and M. S. Seyed Dorraji, Facile synthesis of copper/reduced single layer graphene oxide as a multifunctional nanohybrid for simultaneous enhancement of antibacterial and antistatic properties of waterborne polyurethane coating, *Prog. Org. Coat.*, 2019, **131**, 322–332, DOI: 10.1016/j.porgcoat.2019.02.031.

280 D. I. Lee, S. H. Kim and D. S. Lee, Synthesis of self-healing waterborne polyurethane systems chain extended with chitosan, *Polymers*, 2019, **11**(3), 503, DOI: 10.3390/polym11030503.

281 F. Zhang, *et al.*, A novel and feasible approach for polymer amine modified graphene oxide to improve water resistance, thermal, and mechanical ability of waterborne polyurethane, *Appl. Surf. Sci.*, 2019, **491**(March), 301–312, DOI: 10.1016/j.apsusc.2019.06.148.

282 Y. Guan, *et al.*, Ecofriendly Fabrication of Modified Graphene Oxide Latex Nanocomposites with High Oxygen Barrier Performance, *ACS Appl. Mater. Interfaces*, 2016, **8**(48), 33210–33220, DOI: 10.1021/acsami.6b11554.

283 J. Wu, C. Wang, C. Mu and W. Lin, A waterborne polyurethane coating functionalized by isobornyl with enhanced antibacterial adhesion and hydrophobic property, *Eur. Polym. J.*, 2018, **108**, 498–506, DOI: 10.1016/j.eurpolymj.2018.09.034.

284 P. Zhang, J. Zeng, S. Zhai, Y. Xian, D. Yang and Q. Li, Thermal Properties of Graphene Filled Polymer Composite Thermal Interface Materials, *Macromol. Mater. Eng.*, 2017, **302**(9), 1700068, DOI: 10.1002/mame.201700068.

285 Y. Fu, *et al.*, Graphene related materials for thermal management, *2D Mater.*, 2020, **7**(1), 012001, DOI: 10.1088/2053-1583/AB48D9.

286 W. Kong, *et al.*, Path towards graphene commercialization from lab to market, *Nat. Nanotechnol.*, 2019, **14**, 927–938, DOI: 10.1038/s41565-019-0555-2.

287 *BSI Standards Publication (BS EN ISO 18797-1:2017): Petroleum, petrochemical and natural gas industries — External corrosion protection of risers by coatings and linings*, United Kingdom, 2017.

288 Armorthane, Containment Berms for Oil & Gas Industry, 2020. [Online]. Available: https://www.armorthane.com/protective-coating-applications/industrial-protective-coatings/oil-gas-berms.htm. [Accessed: 24-Aug-2020].

289 F. C. Krebs, Fabrication and processing of polymer solar cells: A review of printing and coating techniques, *Sol. Energy Mater. Sol. Cells*, 2009, **93**(4), 394–412, DOI: 10.1016/j.solmat.2008.10.004.

290 J. Nicasio-Collazo, *et al.*, Functionalized and reduced graphene oxide as hole transport layer and for use in ternary organic solar cell, *Opt. Mater.*, 2019, **98**, 109434, DOI: 10.1016/j.optmat.2019.109434.

291 S. K. Patel, S. Charola, C. Jani, M. Ladumor, J. Parmar and T. Guo, Graphene-based highly efficient and broadband solar absorber, *Opt. Mater.*, 2019, **96**, 109330, DOI: 10.1016/j.optmat.2019.109330.

292 M. F. El-Kady and R. B. Kaner, Scalable fabrication of high-power graphene micro-supercapacitors for flexible and on-chip energy storage, *Nat. Commun.*, 2013, **4**, 1475, DOI: 10.1038/ncomms2446.

